



UiT The Arctic University of Norway

Faculty of Natural science and technology. Department of Physics and Technology, UiT.

Configuring electrochemical 3D printer for PCB production

[A qualitative evaluation]

Vegard Størkersen

Master's thesis in Energy, climate, and environment. Course code EOM-3901. Date [7 2022]

1 Acknowledgment

In this master thesis I had help from Tuza Adeyemi Olukan for looking over the paper, helping in the design of the circuit board and the practical. For use of the traditional machine to cut out the board I should compere I had help from Ståle Antonsen.

2 Abstract

The prime motivating factor for this paper is investigating the new fluid metal 3D printer/etcher. First, given the relatively short entrant of the system into the market, there are little or no resources in the literature detailing the working principle of the system. In this regard, this work will provide an abridge overview of the system, required for interested party to get started. The content off this work will be to compare fluid metal 3D printer to an electro bord printer and see who of them are more sustainable in use. The concluding part of this work summarize key finding of the system assessment with recommendations on how to address certain issues observes during the operation of the system. Addressing some of these issues might accelerate the adoption of this technology by potential end users.

3 Content

Table of Contents

1	Acknowledgment	1
2	Abstract	2
3	Content	2
4	Figure	2
5	Table.....	4
	Concentration of the Electrolytes	25
	Efficacy of the Electrolytes	26
	Concentration of the Electrolytes	31
	Efficacy of the Electrolytes	33

4 Figure

Figure 1: Geeetech i3 pro B 3D printer. Source: <https://www.fluidmetal3d.com/product/.....> 14

Figure 2. Full add-on fitted on the Geeetech i3 pro B 3D printer. Source (FM3D Installation manual).....	15
Figure 3. Main electro-hydraulic circuit. Source (FM3D Installation manual)	15
Figure 4. Filter-Nozzle Assembly. Source (FM3D Installation manual).....	16
Figure 5. Workplace support. Source (FM3D Installation manual).....	16
Figure 6. Peristaltic pump Setup. Source (FM3D Installation manual).....	17
Figure 7. Range extender. Source (FM3D Installation manual)	18
Figure 8. Electronic box and power /signal controller. Source (FM3D Installation manual).	18
Figure 9. Electronic Controller for stepper motors and pump. Source (FM3D Installation manual).....	19
Figure 10: LPKF protomat s62: Link: http://www.lpkfusa.com/datasheets/prototyping/s62.pdf	21
Figure 11: Image of shape. Left original and right, path and etch from Repetier host.	25
Figure 12: Hypothetical Layout	27
Figure 13: magic wand top. Link: https://365.altium.com/files/C61E0E42-C92D-11EB-A2F6-0A0ABF5AFC1B?openedFrom=CMWebsite&variant=%5BNo%20Variations%5D	27
Figure 14: magic wand modified bottom	28
Figure 15: magic wand modified top	28
Figure 16: circuit for the EC3D printer. Shown from repetier host. Made by Tuza	29
Figure 17: FM3D power section	29
Figure 18: FM3D chip section	30
Figure 19: FM3D light section	30
Figure 20: Rounds of program to penetrate 0,5mm copper at a given salt concentration.	32
Figure 21:Initial Etch result using default Scan Velocity and low number etch passage.	34
Figure 22:Possible Effect of low Scan velocity and Partial Etching.....	35
Figure 23: AFM images of PCB surface. Topography (Right) Phase Change (Left).....	36
Figure 24: AFM image used in quantifying the Surface rougenes and Chemical heterogeneity.	36
Figure 25: Battery Power Circuit. Digital copy (Left) FM3D traces (Right)	38
Figure 26: Chip section. Digital copy (Left), FM3D traces (Right)	38
Figure 27: Lighting Circuit. Digital copy (Left). FM3D traces (Right).....	38
Figure 28: Top of LPKF protomat s62 magic wand.	39
Figure 29: Bottom of LPKF protomat s62 magic wand.....	39
Figure 30: Assemphy of components on PCB.	40

5 Table

Table 1: Comparison of technical data between the FM3D and LPKF.	20
Table 2: Optimal Concentration of Electrolytes	31
Table 3: Efficacy of the electrolyte after multiple use.	33
Table 4: Force curves for Figure 24.	37

INTRODUCTION

3D printing is an additive manufacturing (AM) method where a part is constructed layer by layer through deposition technique, melting of powder or chemical binding. This technique has a few advantages over the traditional manufacturing ones. In AM, a digital model of the desirable object (CAD) is developed first and converted to a universal file format (STL or VRML) for 3D printing. The fabrication process is performed with a 3D printer. The 3D printer often deposit layers of materials like polymer, plastic, metal etc in a cyclic manner until the cross section of the object build on top of each other [1]. In addition to the ease of designing the part, the ease of fabricating complex and personalised part at relatively low cost [2] is desirable across the industries. Due to this reason there has been an uptake of this technology across the prosthetics, [3], aerospace, [4], food, [5], and medical [6] industries. While the central core of all AM technique rests on building and consolidating layers principles, the process can be distinguished based on how these processes (building and consolidation) are achieved. For instance some processes deploy thermal energy from laser or electron beams to melt feeder materials, others uses non-thermal technique to spray binder onto powdered ceramic or polymer [7]. As per ISO (ASTM), seven major AM processes has been classified. These processes are **material jetting, binder jetting, material extrusion, powder bed fusion, sheet lamination, direct energy deposition** and **vat polymerization**[8]. However, in this work, AM processes are classified as selective layer sintering (SLS), Stereo lithography (SLA), Laser engineered net shaping (LENS), Laminated Object Manufacturing (LOM), Fused deposition modelling (FDM) and Electrochemical additive manufacture (EAM).

SLS offers the flexibility to rapid produce complex, personalized parts that provides better durability and functionality over other AM processes. In SLS, a powder is sintered with the aid of laser beam. In specifics, the laser beam binds the powdered particles together (pre-determined by the sliced design). The advantage of this technique is that is suitable for a variety of materials. In the literature, authors have reported this technique on plastics, metals, composition of different metallic materials, hybrid of polymer and metal, ceramic and hybrid of metal and ceramics [9, 10]. Another noteworthy trait of this technique is the relative fast build time and the absence of post curing procedure. In addition, unused feedstock materials can also be recycled thereby reducing material wastage. On the other hand, SLS operation can be complex with poor surface finishing compared to other AM techniques. For instance, in

order to prevent oxidation during the building process, the operation is performed in an gas atmosphere and constant temperature at the melting point of the material. Also, the particle size of the powdered feed material can be a limiting factor in the SLS operation technique.

SLA employs photo polymerization of liquid resin (with the aid of UV laser) in building printed parts. The laser beam traces out and hardens the pattern of the desired part on the resin's surface. This procedure is repeated for all sliced layers of the desired parts. The processes of building described earlier is detailed in [11]. The benefit of this technique over other AM is the rapid build time and good surface finishing. These traits make the technique more suitable technique in the manufacturing industry. Some of the downside of this technique includes the need for support structure while printing and post processing time and resources required to remove the structure. In addition, the cost of processing, materials and machine are notable barriers of this technique. Accessibility to the feed materials in SLA might be limited[12].

In the LENS technique, metallic powdered materials are liquefied (using powerful laser) and infused into a particular area. As in the SLS technique, the solidification process (the liquefied material) needs to be performed in an inert environment to eliminate oxidation. Typical feed material that can be deployed in this process includes stainless steel, copper, titanium, alumina etc. Due to the design nature of this technique, it is more suitable for repairing damage parts or producing the whole part for replacement. The downside of this technique is that the process of heating and cooling can lead to issues related to residual stress in the printed part. The presence of residual stress in some machine parts can lead to premature failure of the machine. Furthermore, LENS can lead to uneven surface finishing thus requiring post processing procedure to smoothen the surface.

LOM is a unique AM technique because of the combination of both additive and subtractive processes in the fabrication of parts. The additive part includes gluing materials thin layer of material together with the aid of pressure, heat and adhesive coating. The subtractive part includes using laser beam to cut out the desired shape. This process has the advantage of eliminating the concerns of residual stress as expressed in LENS. Also, the need of support structure is not required thereby reducing the need of post processing technique. It is also feasible to design the printer for the fabrication of large parts. All these possibilities make the procedure a low-cost one and thus one of the favourable for budget conscious users. In addition, this technique can be deployed on a number of materials. Some of the demerits of this technique has to do with the subtractive process. This is particularly pronounced with parts with intricate

internal cavity. Also, the poor surface finishes and accuracy of the printing techniques limit the deployment of the technology in industries with little or no need for precision.

The FDM is one of the most versatile AM techniques due to its relative simplicity. In this technique, feeder wire-like material (thermos plastic filament) is inserted into a nozzle head. The nozzle head with fitted heating filament liquefied the filament to a temperature a little bit above the melting point and extruded through the nozzle head. The head is rasterized around the printed area in conformity with the CAD file pattern. The extruded material from the head solidifies almost instantly on touching the printer bed (first layer) or cold weld on existing layer. Possible materials for this process includes polycarbonate, acrylonitrile butadiene styrene, ceramics, metal and casting wax[13]. Also, the possible of using hybrid materials or additional reinforcement can be implemented using multiple nozzles in the printer head. Depending on the design choices, high printing resolution and accuracy can be obtained. Also, FDM design can be compact, robust and offers low-cost 3D printing solutions. Possible downsides is the low surface finishing, additional requirement to smoothen the surfaces and requirement of removing the support structure after printing.

EAM is a relative new AM technique compared to earlier examined processes. In addition, this technique is most suited for 3D printing of metallic parts. The process includes the deposition of tiny and highly adherent of metal onto a the surface of conductive substrate through the reduction of metal ions in an electrolytes [14]. There are variant form of this technique, and this subject will be further explored in details in the subsequent section of this work. In specific this work intends to examine the efficacy of a new variant of EAM in the fabrication of electronic parts. For simplicity, the work will document the performance of the EAM in the rapid fabrication of printed circuit board (PCB). The EAM fabricated board will be benchmarked against one produced by a commercialized PCB making machine. Hence this thesis will be structured as follows. First, given the relatively short entrant of the system into the market, there are little or no resources in the literature detailing the working principle of the system. In this regard, this work will provide an abridge overview of the system, required for interested party to get started. Overview of the proposed EAM system will be examined. Methodology of the designed experiment and assessment procedures, using the proposed EAM system will be detailed. The concluding part of this work summarize key finding of the system assessment with recommendations on how to address certain issues observes during the operation of the system. Addressing some of these issues might accelerate the adoption of this technology by potential end users.

Literature Review

Addictive manufacturing in electronics

In recent times, AM is making inroad in the electronic space for fabricating various high-end performance and flexible electronics[15-29]. In the literature, the phrase printed electronics is synonymous with components produce by AM technique. For consistency, this work refrain from using the term and stick to the AM. AM in electronics will play a key role in future electronics and has been referred to as the next frontiers in additive manufacturing and printed electronics[8]. More often, this technology has been used in the printing of electronic traces and interconnectors, resistors, inductors, capacitors, radio frequency identification (RFID) tags, disposable electronic components, and energy storage devices to name a few. Also, AM holds promises in the production of emerging products like embedded and stretchable electronics. Reason for uptake of this technique in this field can primarily be linked to the high throughput in production and flexibility of customization. In addition, this technique holds promise in the fabrication of complex electronic components with multiple functionalities. Usually, the deposition or embedment of electronic components 3D structure to form a multi-functionality product is achievable by interrupting the 3D printing process. This is made viable by the layer-by-layer working principle of AM. Hence, smart structure markets, application and opportunities are looming as sensors and circuitry can easily be integrated in conventional 3D products. A major challenge however is that, from the literature perused there is absence of standardize method to achieve the lofty potentials of AM in electronics.

For instance, Yue et al. in [30] demonstrated the capability of 3D printing technology for power electronic converters [31]. Also the authors claim the heat sinks produced with their technique is relatively cheaper than the conventional system with high conductivity, [32]. Other devices like power inverter, [33], air core inductors, [34], heat pipe, [35], and circuit board, [30] show similar superior properties. In their work, they compared certain components, like printed circuit board (PCB), power inductor for a buck converter and a heat sink, produced from a 3D printer with a commercial milling machine. Even though the authors acknowledge the potential of 3D printing technology in the electronic industry, but they expressed limitations related to materials. Flowers et al. in [36] examined the utilization of fused filament fabrication (FFF) for 3D printing electronic components with thermoplastic filaments. In the thermoplastic filaments

used in the study, carbon-black, graphene and copper were used as conductive fillers. Although the authors successfully demonstrated the potential of their technique for printing electronic components, the machine setup can be relative expensive and requires complex machine setup.

In the literature, other authors have achieved advance functionality in 3D printed structures by intermittently stopping printing processes and incorporating the electronic structure. For instance, building on this ideology, a CubeSat Trailblazer (with embedded electronics) has [37]been launched[38-41]. As hinted earlier, this setup was achieved through the assemblage of complex manufacturing setup. Specifically, this setup included two FDM systems, computer numerical control router (CNC) and precision dispenser for conductive ink. This elaborate setup makes this system outside the reach of most consumers and hobbyists and more suitable for well-funded research institution. Another technique was deployed in [42] to demonstrate the viability of AM technique for electronic structure. In the work, the authors manufactured a shoe insole embedded with sensors (pressure and temperature) and wireless communication chip. The project was accomplished with a combination of multi-materials from ink jets, aerosol jets and extrusion print heads. Similar technique was demonstrated in [43] to fabricate a “smart cap”(SC). The SC was embedded with sensors and deployed to monitor the state of liquid food wirelessly. While both projects successively demonstrated the capabilities of their proposed techniques at the lab-scale, this technique might be not be feasible in the field. First material requirement for both setups might be limited and exorbitant. Also, there might be health concern regarding the incorporation of electronic structures in food consumables.

In [44, 45] authors combined stereolithography and direct print technique to produce embedded electronic 3D structure. Stereolithography was used to fabricate the holding mechanical structure while the interconnections between the electronic components can be made with direct print conductive inks. These techniques have been used to fabricate functional 2D and 3D 555 timer circuits. However, the technique consisted of using customized designs rather than the commercialized design. In order to circumvent the manufacturing complexity associated with printed circuit board Jiang et al.in and Lopes et al. in [44, 45] demonstrated a hybrid process using stereolithography and direct writing technique. While various authors have demonstrated the possibility of using multiple material in 3D printing of electronic structure no study is done to access the durability of these devices. For instance, there has been concerns about contamination issues with deploying multiple viscous materials in a s single build. Also, the materials deployed are limited, while conductive ink with low-temperature curing capabilities is still an issue[7]. In addition, there are lean studies detailing the interfacial conditions between

different materials. More specifically, phenomena like surface wettability, surface roughness, material compatibility and force of adhesion play critical role in interfacial conditions, but these conditions have not been factored in any of this demonstration.

Electrochemical 3D printer

As perused in the literature, most of the application of AM in the electronic industry relies on polymer filaments, with conductive filaments. Due to this, the most common 3D printer is the FDM [46]. Recent advances in technology have made it viable to use metal material for printing. With the metal 3D printers, FDM technique is still one of the most predominant techniques. The FDM, using a metal filled polymer filament, where metal powder in a polymer is fused together when the polymer (including the powder) sublimate, [46]. Other common processes are direct metal laser sintering (DMLS), where a powder in a container is melted by laser, [47], electron beam melting (EBM), similar to metal laser sintering but uses a beam of electron instead of laser, [48], directed energy deposition (DED), the powder is sent into an energy beam where it melts and form the part, [49]. While DMLS, EBM and DED are versatile the downside is the heat and energy requirement to melt or partly melt the metal powder needed to construct the part. Also, the FDM need heat to sublimate the polymer holding the powder. To address the issue of heat and energy requirement, most people have explored the option of electrochemical metal 3D (E3D) printing technology. This is due to the fact that E3D printer can deposit metal at room temperature [50]. Also, this technology offers a simple and relatively inexpensive way to develop metal parts (especially in the microscale) compared to other 3D techniques mentioned earlier. E3D is AM technique that uses principle of electrodeposition (ED) or electro-etching (EE) to generated 3D structures with the aid of an electrolytes. Electrodepositions refer to the process where ion in an electrolyte builds up on a conductive surface due to the process of reduction. Electro etching will refer to the process where a certain part of a conductive surface oxidizes at the impact of an electrolytes. In 1996 by J. D. Madden and I. W. Hunter where demonstrated the principle of electrochemical 3D (E3D) by having a sharp anode close to the build plate (cathode) to localise the deposition, [51]. Subsequent authors have demonstrated the capability of this process by using it for making sub-micron electronics interconnection, [52], and a dip-pen method for printing [53]. The technology has

also been demonstrated with platinum as printing material [54]. The Metal 3D market is expected to swell to \$21 billion and E3D is expected to form a major market share. In 2020 according to a work the paper from 2019 “Metal 3D printing in construction: A review of methods, research, applications, opportunities and challenges”[55]. While there are several techniques discuss in the literature to achieve this process, in this work emphasis will be on the variant form introduced by Fluid Metal 3D (FM3D) [56]. The FM3D [57] is a novel electrochemical 3D printing system recently introduced into the market [58].

In the proposed system by FM3D, a ‘fast ‘emitting jet of electrolytic solution impacts an electrically conductive target substrate for ED process. Emphasis needs to be placed on the ejection speed of the emitting jet as this is crucial for circumventing the barrier associated with E3D. It has been reported that the deposition rate and the size of the printed features are limitation of E3D. The deposition rate is tied to the development of diffusion layer forming in the proximity of the cathode[59]. The fast electrolyte moving jet disrupts the diffusion layer thus increasing the rate of metal deposition. In addition, the rate of deposition can also be controlled by the modulation of applied voltage between the electrodes. However, increase the voltage beyond certain limit might lead to the formation of dendrites and thus affect the morphology of the printed objects. In this respect finding the optimal voltage setting is crucial for precise metal deposition. Inverting the voltage of the setup will oxidize the substrate (etch) as hinted earlier. Therefore, with the modulation of the applied voltage between the electrodes the possibility to continuously switch between from local deposition to localized removal is presented. These traits make the FM3D ideal for performing complex 3D metallic structures and electronic components as well.

A particular noteworthy design of the FM3D The system capitalizes on producing kits that can be used to reconfigure conventional FDM commercial 3D (polymer) printer into metal 3D fabrication. In one of the versions of the product, the firm demonstrated the modification of Geeetech i3 pro B 3D printer [60] for metal printing purposes. A big plus to the electrochemical 3D printing technique is the ability to carry out subtractive manufacturing (SM) without the need of changing setup or disrupting the operation of the system. The FM3D system also has the capability to perform both additive and subtractive operations. The removal of material is achieved by reversing the polarity of the voltage [61] as explained earlier. Building on this capability FM3D was also designed to give a real-time, closed loop feedback functionality. This

ensures that build quality can be control in situ. In addition, the relative simplicity of the technology means that ‘cheap’ convention 3D printers can be retrofitted with FM3D part component easily and operated with little or no training required.

Printed Circuit Board (PCH)

PCB was invented 1903 by Albert Hanson as a concept of a laminated foil onto an insulated board in multiple layer [62]. Ancient PCBs were manufactured by use of drilling holes and inserting wiring called through hole construction, [63].After 1949 a method called auto-Assembly process where components are soldered into the plate was invented by Moe Abramson and Stanislaus F. Danko, [64].During the late 1970 and early 1980 the complexity of the PCB increased to the point where the need to test the board became important in quality testing [65]. Recently the use of 3D printers have been used to make PCB, [62]. Today the amount of PCB sold each year has a value of \$1 trillion, [66].Some machine at the market are Voltera v-one, [67], Kayo-5088XL, [68], and PCB board baking machine [69].

Gap Addressed in This Work

While the capability of 3D electronic printing has been demonstrated and established in the literature, there are certain issues observed in some the perused work. First, most setup used to achieve this purpose consist of hybrid combination of various printing technology. The hybrid combination often results into to complex, costly and elaborate setup with “steep” learning curve. Thus, most of the demonstration are suitable for lab-scale deployment and impractical to deploy in the field. Also, the material required for this purpose could be toxic, costly, non-environmentally friendly and restricted to certain manufacturer.

Also, another traditional way of fabricating PCB for prototyping is through the mechanical milling of PCB sheet. This technique shows clear benefit over the commercial PCB chemical manufacturing technique. These benefits include, affordability, smaller footprint size, lack of chemical during etching, quicker time from conceptualization to fabrication, supports in house

production and relatively easier to operate. However, from the literature perused and it remains to be tested against the FM3D.

This work intends to deploy the FM3D in fabricating a PCB for electronic device manufacturing. Precisely, the following area will be addressed in the work.

1. The conversion of conventional FDM machine into metal 3D printer machine with the FM3D kits.
2. The optimization of the working parameters suitable for the arctic climatic condition.
3. Production of PCB from the setup
4. Benchmarking the produced PCB with product from commercial PCB milling machine.
5. Result and discussion of the benchmarking
6. Recommendation for future iteration of the system

The motivation for selecting FM3D in this study can be listed as follows:

- a. Simplicity of the machine architecture and set up.
- b. Relative low cost
- c. Requires no special training to operate
- d. Non-toxic electrolytic material. For this water a salt and water electrolyte will be deployed for the PCB production
- e. Easy maintenance as the part can be access by the user and troubleshoot
- f. Most of the kit can be replace by 3D printing as far as the digital model is available.

Although, while the machine can be used for both EP (addictive) and EE (subtractive) purposes, for the work, only the EE process will be carried out. The main reason for this is due to the need to benchmark the product of this machine with the commercial *milling* PCB machine. This is essential to match the nature of the operation (etching vs milling). Also, depositing copper on a non-conductive insulated board requires specialized setup (will be addressed in subsequent session) which defeats the one of the purposes of this work. i.e. materials used should be easily accessible.

FM3D printer Set-Up and Operation procedure

The major kits (hardware add on) required for this conversion are shown in Appendix 1. The key components in the kits are the nozzles with filter, electronic box, the pump, pipes, tray and supports. The process of retrofitting the Geeetech i3 pro B 3D printer is illustrated from Figure 2 to Figure 9. The images are also annotated detailing the add on fittings and installation steps. The operation procedure of the machine is detailed in Appendix 2.

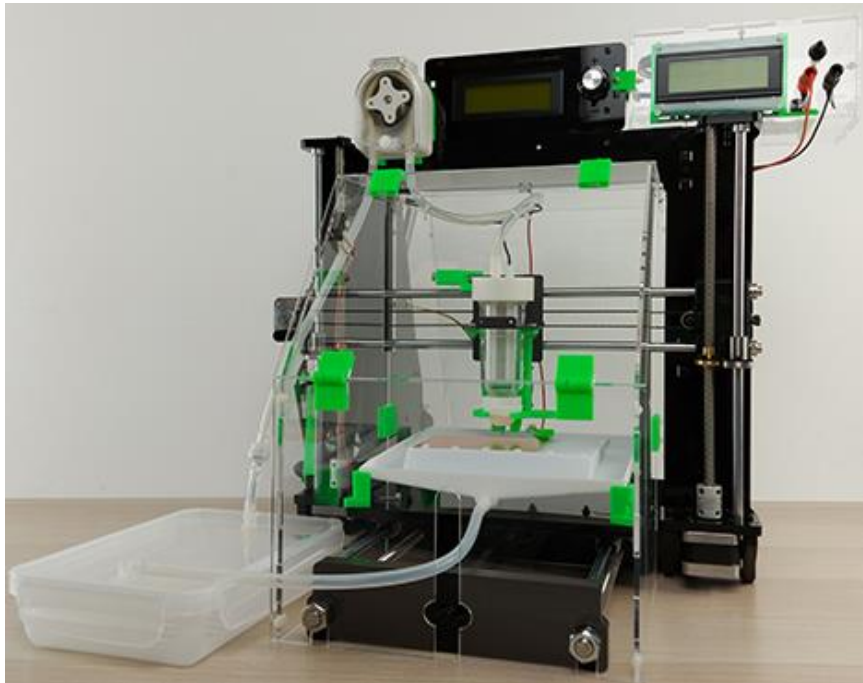


Figure 1: Geeetech i3 pro B 3D printer. Source: <https://www.fluidmetal3d.com/product/>

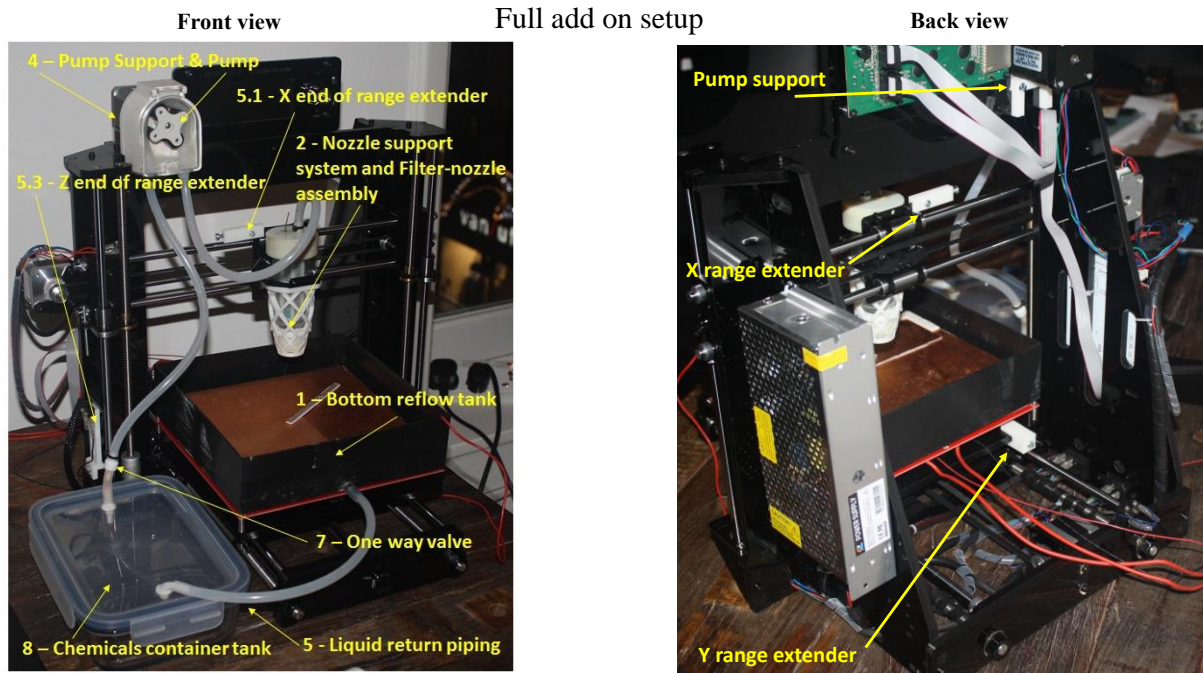


Figure 2. Full add-on fitted on the Geeetech i3 pro B 3D printer. Source (FM3D Installation manual)

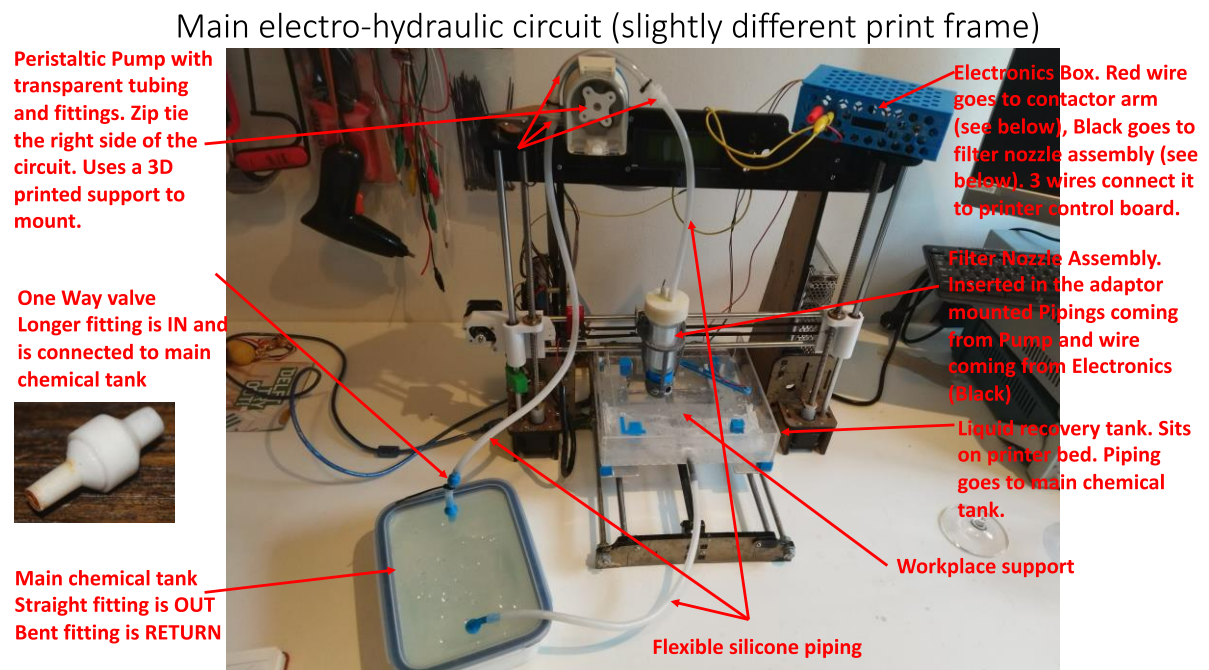


Figure 3. Main electro-hydraulic circuit. Source (FM3D Installation manual)

Filter-Nozzle assembly

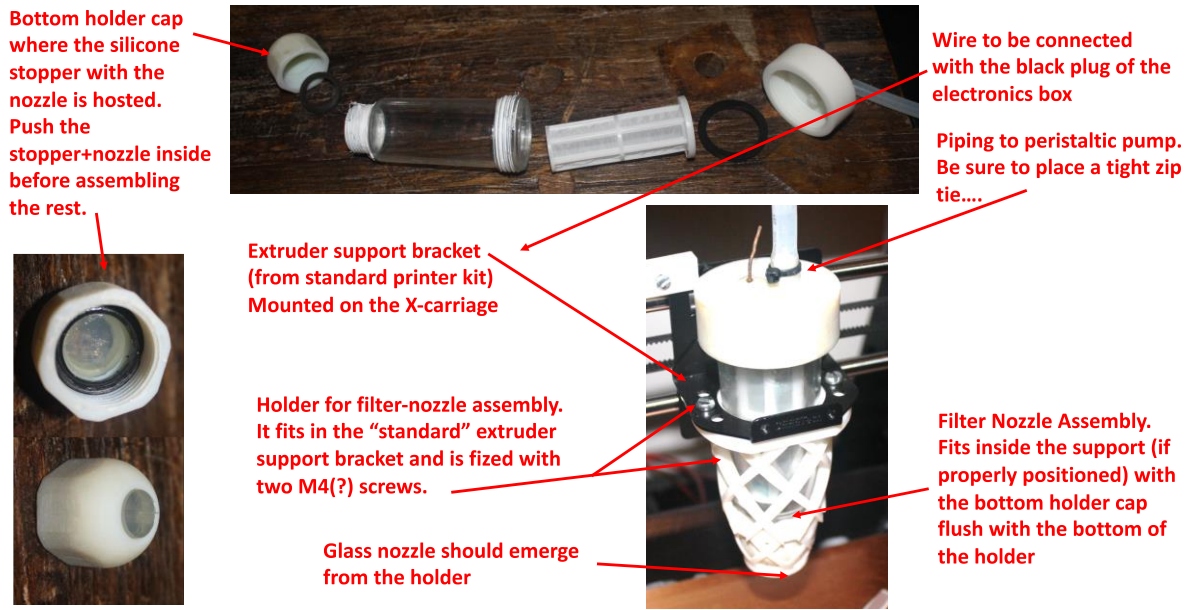


Figure 4. Filter-Nozzle Assembly. Source (FM3D Installation manual)

Workplace support

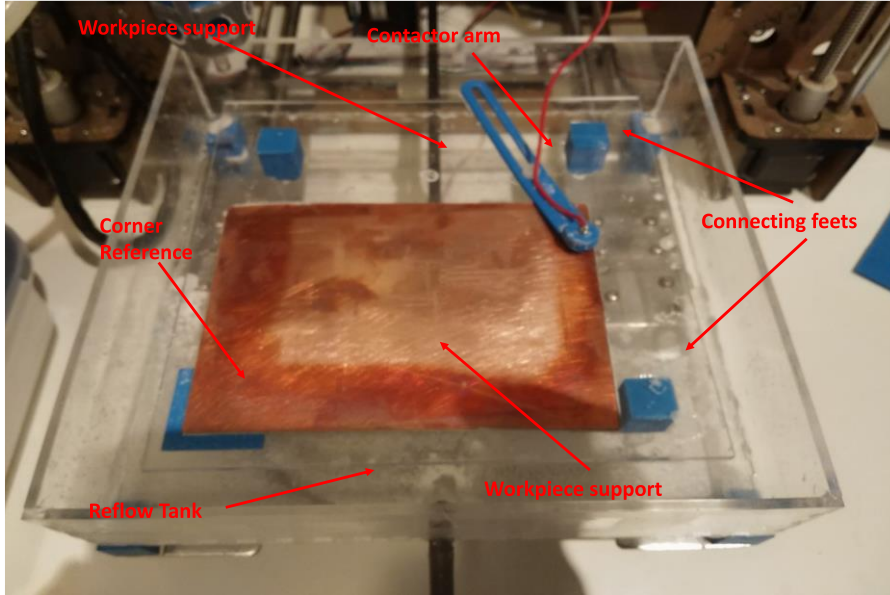


Figure 5. Workplace support. Source (FM3D Installation manual)

Peristaltic pump

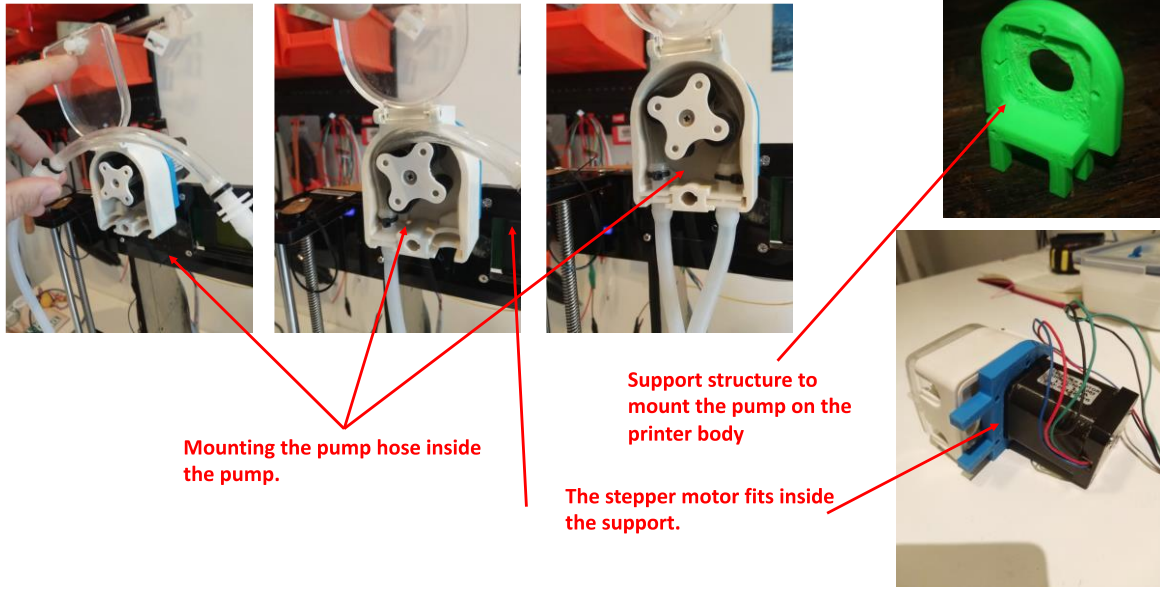


Figure 6. Peristaltic pump Setup. Source (FM3D Installation manual)

Range extenders

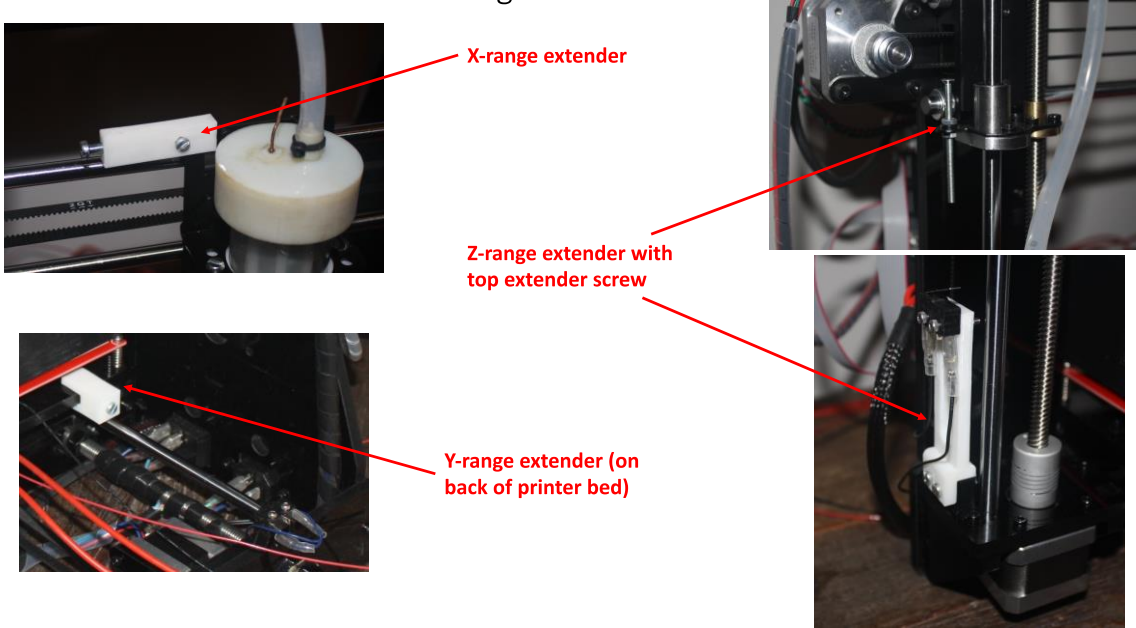


Figure 7. Range extender. Source (FM3D Installation manual)

Electronics

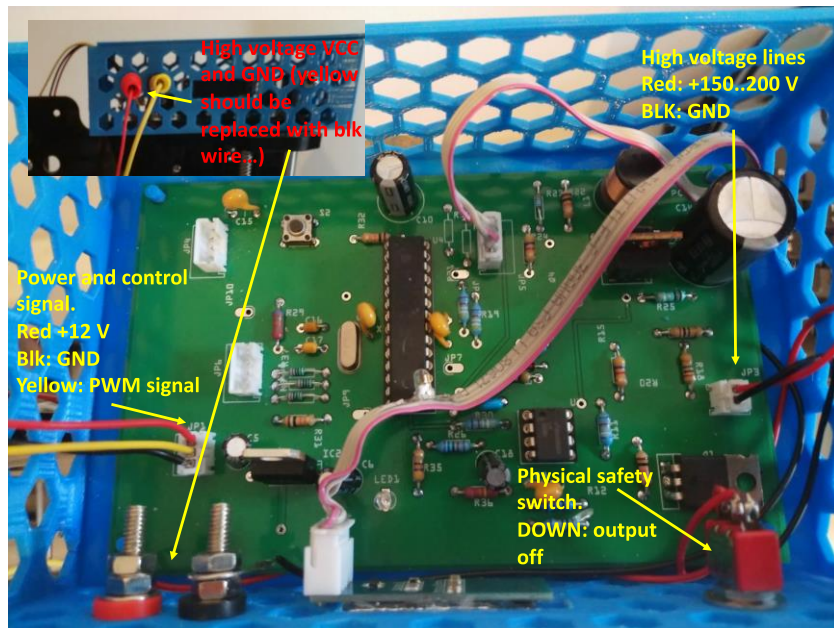


Figure 8. Electronic box and power /signal controller. Source (FM3D Installation manual)

Electronics

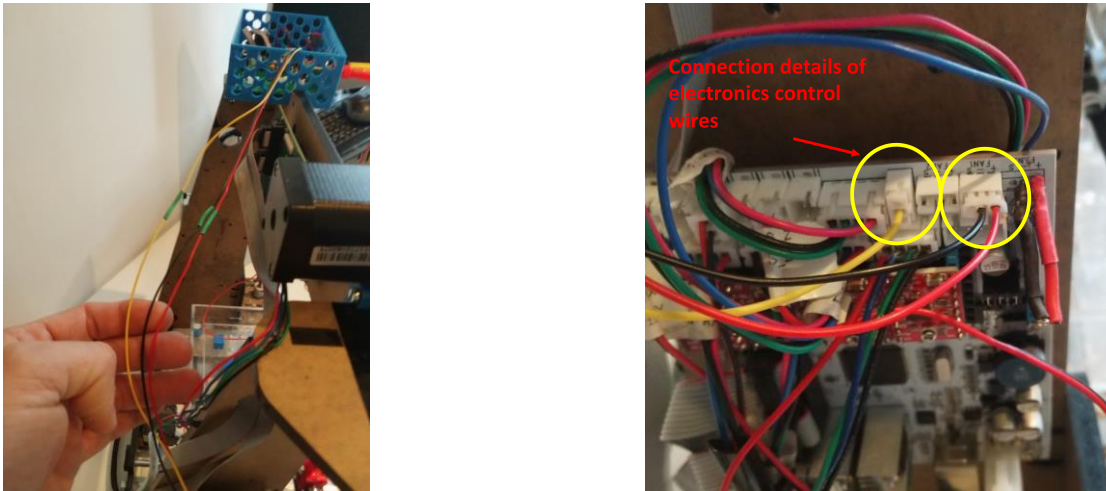


Figure 9. Electronic Controller for stepper motors and pump. Source (FM3D Installation manual)

LPKF milling machine and Operation procedure

The LPKF ProtMat S62 (LPKF) is a PCB milling machine also known as isolation milling. This process is referred to as isolation milling because the system is designed to create electrical isolation on the original PCB sheet. In essence, the machine works by mechanically removing area of copper materials from a sheet of PCB. The material removal follows a predefined pattern (from the digital layout) to recreate pads, traces, and structure [70] required to achieve a design functionality. While the process of material removal is different from the FM3D printer, they can be both grouped as subtractive process. Another similarity between the LPKF and the FM3D is portability of the system and can be operated in a confined environment without elaborate setup. The accuracy of the machine is dependent on the milling bits and their respective cutting/rotational speed as well as the milling accuracy and control. The technical specification of the machine is presented in the table below. The setup of the system and operating detail is contained in [71]. Unlike the FM3D, training is required to get acquainted with the system and operation is more tasking than the LPKF.

Table 1: Comparison of technical data between the FM3D and LPKF.

	FM3D	LPKF
Power Consumption	120 W	200 W
Weight	10 kg	55 kg
Dimension (W x H x D)	550 mm x 600 mm x 600 mm	670 mm x 540 mm x 760 mm
Operating Temperature	15°C – 25°C	15°C – 25°C
Allowed Humidity	Not Specify	60 % Max.
Tool Change	Manual	Automatic
X/Y-drive	Step Motor	3-Phase Motor
Z-drive	Step Motor	Step Motor
Smallest Drilling Diameter	50 um	200 um
Noise	54 dB	71 dB
Cost	Less than \$1,000	\$ 10,000 +
Multilayer	Single Layer	Double Layer Circuit
Etching Method	Electrochemical	Mechanical
Post Processing	Required	Not Necessary
Operating Software	Proprietary	Proprietary
Working tool	Salt/Water Electrolyte Jet	Drill bits

While the LPKF might have clear advantage over the conventional PCB chemical manufacturing technique, it remains to be tested against the FM3D. However, one clear advantage of this system with the FM3D is the presence of automatic drill for hole making. FM3D requires the setup of high precision drilling system.



Figure 10: LPKF protomat s62: Link: <http://www.lpkfusa.com/datasheets/prototyping/s62.pdf>

Methodology

According to the manufacturer, the LPKF is marketed as a compact high-speed plotter with high precision and performances for fast and easy milling and drilling circuit board prototypes. The system is expected to deliver in-house PCB prototyping promising users faster design to market when compared to the conventional route. The faster delivering time is hinge on the prospect of circumventing the delay associated with outsourcing PCB prototyping with outside vendor.

Given these attributes, the work aims to benchmark the FM3D against the LPKF machine. This is pertinent because the FM3D (etching process) can perform similar capability. However, as shown in Table 1, the FM3D shows superior advantages in area of cost, lower noise, drilling resolution, weight, and power consumption. However, it will be challenging to benchmark the two machines based on the production speed. This is due to different in capabilities of both systems. While the LPKF can work on multilayer PCB, the FM3D is limited to single layer PCB.

Also, the optimal setting of both systems. For instance, during this work, for a particular design, the time range of the LPKF ranged from 1 hour to 72 hours based on the Gerber file (Circuit CAD design) while the estimated time of the FM3D ranged from 6-12 hours. To avoid the complication and technicality of benchmarking both systems with time, the emphasis of the work is to compare the performance of both systems will be a qualitative assessment of both systems. Specifically, the systems will be adjudged based on the following parameters.

Effective Isolation: The essence of etching is isolating the copper metal from the non-conducting layer pad insulation. Therefore, for a complete operation, it is necessary that area marked for isolation are completely removed. Inability to carry out complete isolation might lead unwarranted short-circuiting and consequently undesired performance of the electronic device. Hence, the capability for system to perform this duty is a top priority for both systems.

Quality of trace/Isolation: This parameter intends to quantify the accuracy of the etch path. This is crucial with traces in proximity. One factor that affects this trait is the vibration introduced in the system during the etching process. Systems with high vibration might require special setup or operating environment. This might lead to secondary cost or additional cost to the machine. Also, the evaluation of this property might determine the ability of the systems to function properly in domestically.

Quality of surface finishing: The surface finishing evaluates surface modification of the PCB after the etching process. It is critical to quantify this property especially for the FM3D due to the nature of the reaction. This property might affect additional secondary process like soldering on the PCB.

Post processing: it will be essential to evaluate the post processing of both systems to be able to quantify the cost and resources required.

Ease of drilling holes: The LPKF comes install with automatic drilling systems and tool. On the on the other hand, getting a through hole with electrochemically is not feasible for PCB due to the insulating pad in of the board. In this sense, this work will evaluate the requirement and setup for manually drilling holes in the PCBs fabricated from the FM3D.

Ease of soldering: Soldering is crucial for joining the electronic components with the fabricated PCB. Improper soldering might lead to issue of short-circuit and undesirable performance of the designed electronic devices. Factors that will determine the process are potential modification of the PCB surface. Also, the size of the padding along the traces is essential. While wider pad around the trace will be preferable and easier for manual soldering, this will likely increase the operational time of the system. Also, this increases the footprint size of the PCB. Narrow padding around the trace on the other hand will lead to compact PCB size but will complicate the soldering process.

Experiment Design

Prior to working with the PCB, the board is placed in a container filled with vinegar for 30 minutes and metal sponge is used to scrub the surface. Alternatively, the copper surface can be covered with salt or lime juice and scrub as well with iron sponge to get rid of potential oxide layer on the copper surface

For the study, this work intends to etch out a PCB layout based on the digital model of the 'magic wand' by Andre Lamothe [72] in Figure 13. The 'magic wand' works by turning on several Led light sequentially. The timing and switching function is controlled by a micro controller chip. The 'wand' should be powered by AAA battery and equipped with potentiometers to adjust the current in the circuit. The complete part list of the 'Magic wand', specification and manufacture type can be found in appendix 3. The motivation for selecting this model, is to test the efficacy of the system against the need of a potential user. Andre Lamothe is a hardware engineer and well known among the DIY communities. As hinted earlier, based on the build bed size of both systems and for optimal printer setup, the model has been modified within this constraint. The adjusted model for the LPKF has two sides top and bottom layer shown in Figure 14 and Figure 15.

Similarly, the digital design was modified to fit within the limitation of the FM3D's printer bed at 15 by 15 cm as shown from Figure 17 to Figure 19. As hinted earlier, due to the limitation to just a single layer etching the digital model of the wand had to be redesigned (same component list) using easyeda software (see appendix 4).

For the experiment, the LPKF was operated as directed as instructed by the operation manual using the default setting. However, the FM3D needs to be turned or calibrated after the assembly. Specifically, the reason for the calibration is to find the right combination of variables that we lead to optimal etching. The variables that can be controlled are

- Concentration of the electrolytes
- Efficacy of the electrolytes over time
- Scan Velocity (mm/min) – Etching Speed
- Travel Velocity (mm/min)- Speed between etching zones
- Etch Current (mA) – Electric charge on impact zone
- Pump Speed (cc/min) – The pressure and liquid volume coming out of the nozzle

- Numbers of Etching Passages – How many times the pattern should be repeated

Concentration of the Electrolytes

The experiment is designed to find the correlation between the concentration of the electrolytes and the etch rate. The electrolytes is made from a solution of table salt and distil water (tap water can also be deployed). The percentage of salt, in a fixed volume of water, was increase while the rate of copper removal was observed. The copper substrate used for this experiment is 0.5mm thick. For each iteration of the experiment, the time, the number of etch passages required to through the substrate is recorded. With these parameters, the average cut per etch passage (etching rate) can easily be calculated. Other parameters (that can be tuned from the interface of the FM3D software) used for this setup are as follows.

- Scan velocity :10 mm/min
- Travel Velocity: 300 mm/min
- Etch Current: 20 mS
- Pump speed: 1000 cc/min

Note these values were chosen arbitrarily and kept fixed for all the different concentration of electrolytes used in the experiment. Also Figure 11 shows the path intended to be etch out.

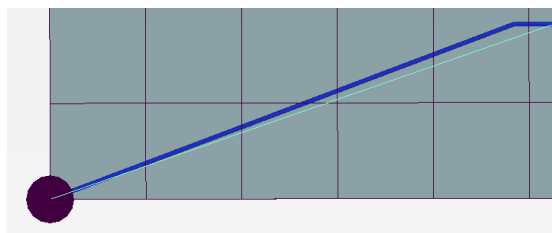


Figure 11: Image of shape. Left original and right, path and etch from Repetier host.

Efficacy of the Electrolytes

Based on the determined optimal concentration of the electrolytes, it is also pertinent to test the efficacy of the electrolytes after multiple etching operation. Particularly, the aim is to observe the effect of the copper ions accumulation (from the dissolved PCB) in the salt -water solution's efficacy in etching. For this test, the system was run multiple time while recording the rate of material removal for each etch passage.

Scan Velocity and Numbers of Etch Passages

The scan velocity determines the etch rate and the number of etching passages. Increasing the scan velocity reduces the etching rate, thus the number of etching passages we need to be increased to compensate for the material removal. The number of etch passages on the other hand determines the number of repetitions for a particular trace before moving to the next trace for a given work. For instance, given the traces (**A** and **B**) in the hypothetical layout in Figure 12 for a given scan velocity, assuming the number of etch passages required to completely cut through is **P**, then the system will move through trace **A** **P** number of times before moving to trace **B**. Alternatively, another system could be operated by setting the number of etch passages = 1 and run consecutively in **P** number of times. In the alternate scenario, the system will run through the traces **A** once before moving to trace **B** with the sequence repeating until the **P** times. Choosing the number of etch passages is also vital and might determine the quality of print for PCB etching.



Figure 12: Hypothetical Layout

Etch Current (mA)

The Etch current is the number of electric charges impacting a zone. With other things being fixed, increasing the etch current should increase the etch rate until an optima value is reached.

Using optimal settings from the experimental setup, the layout of the “Magic Wand” was etched out from the PCB. The PCB used in this work is 0.7mm thick with 17.5um of copper.

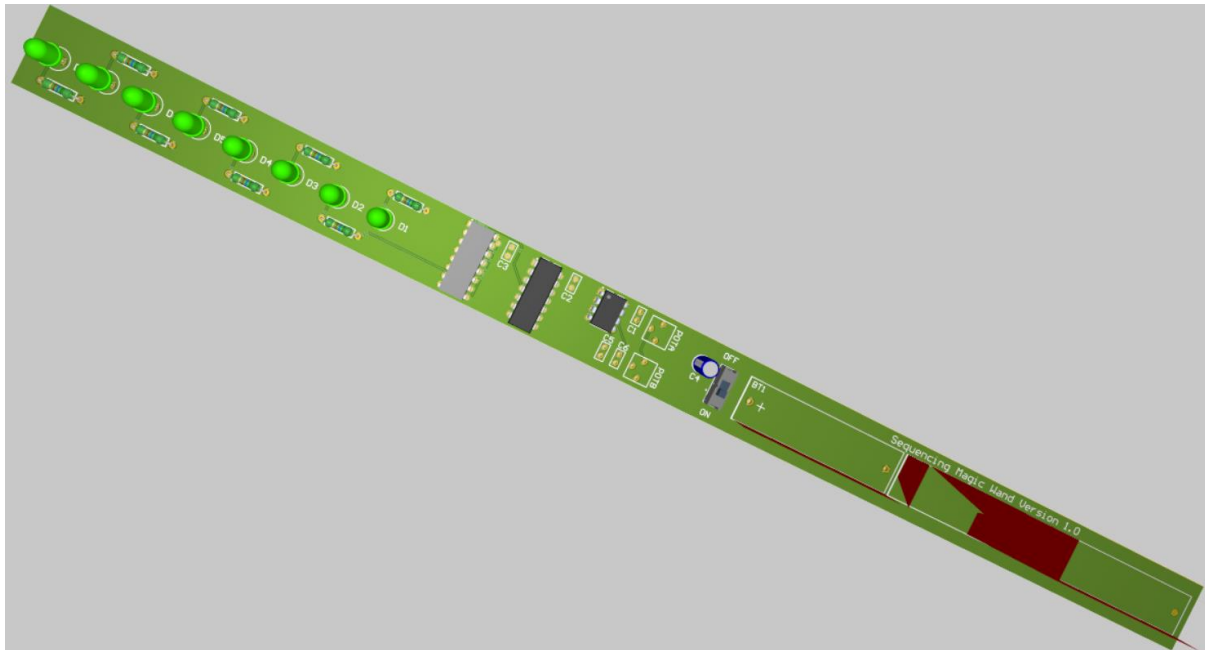


Figure 13: magic wand top. Link: <https://365.altium.com/files/C61E0E42-C92D-11EB-A2F6-0A0ABF5AFC1B?openedFrom=CMWebsite&variant=%5BNo%20Variations%5D>

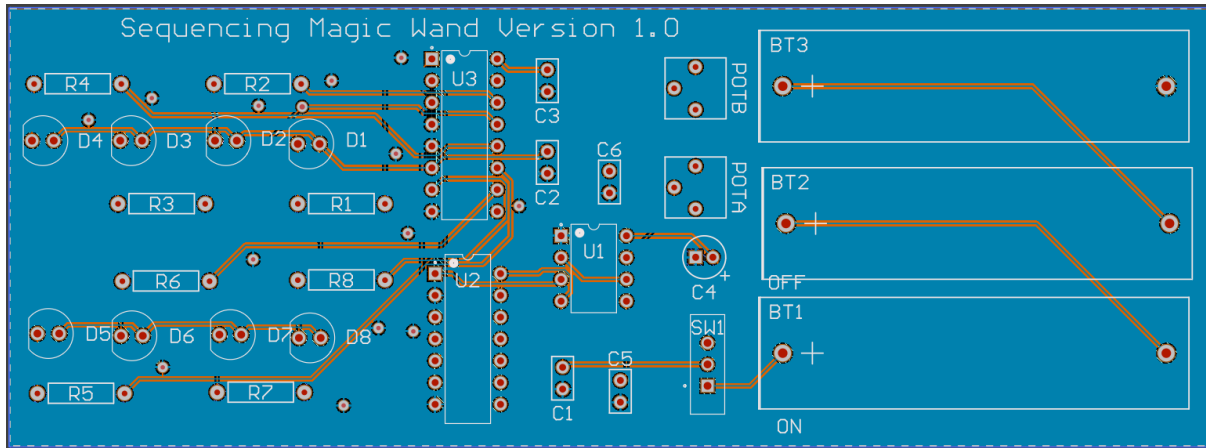


Figure 14: magic wand modified bottom

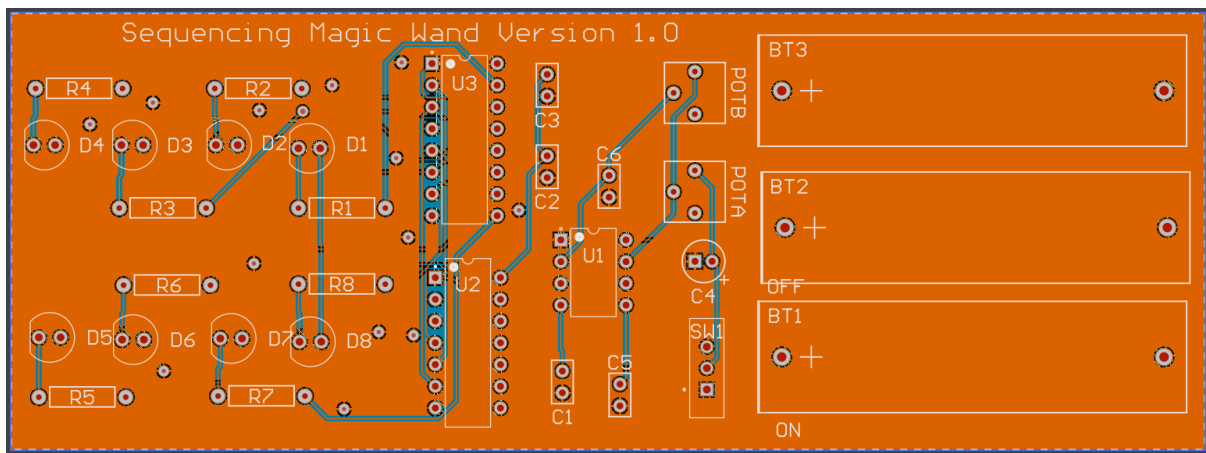


Figure 15: magic wand modified top

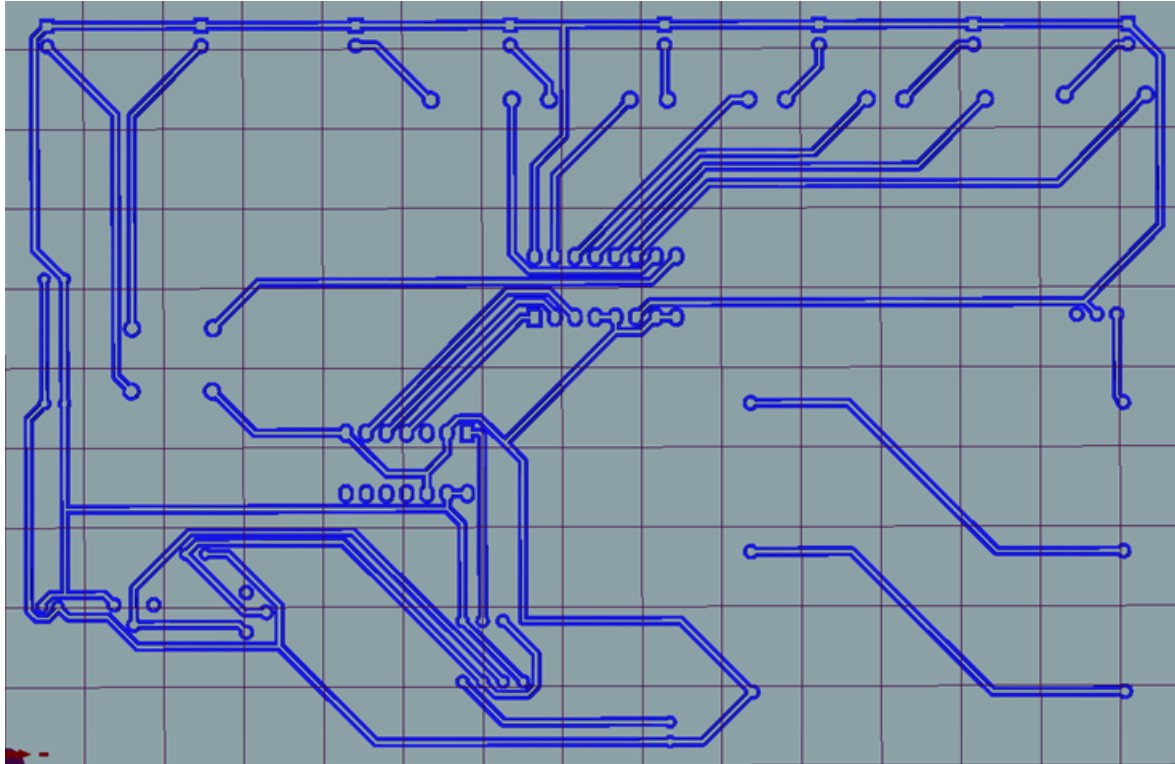


Figure 16: circuit for the EC3D printer. Shown from repetier host. Made by Tuza

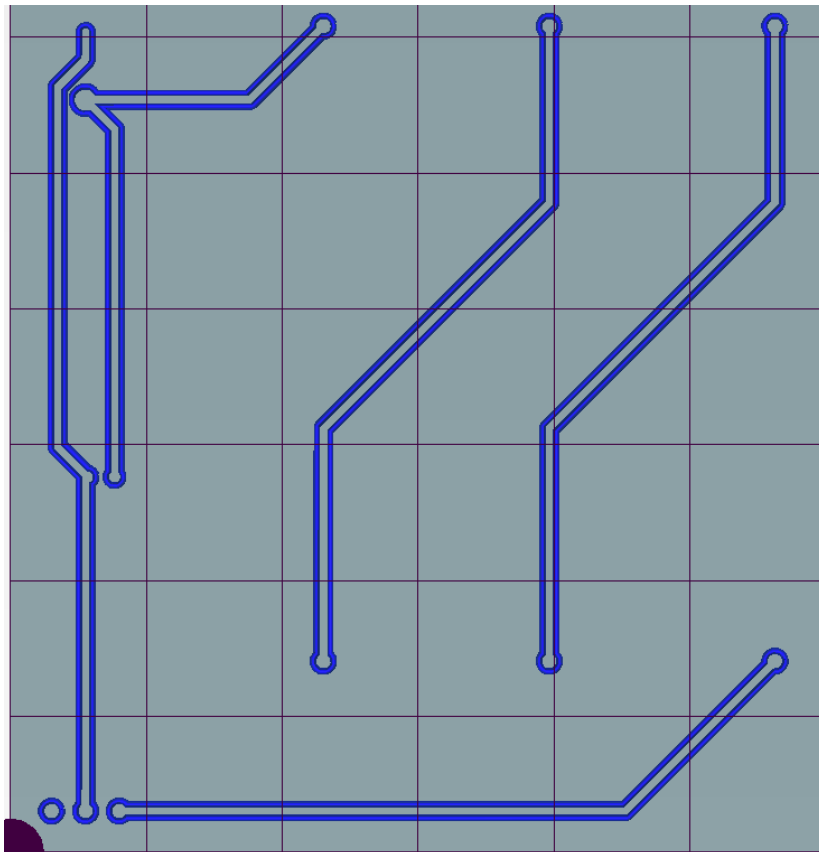


Figure 17: FM3D power section

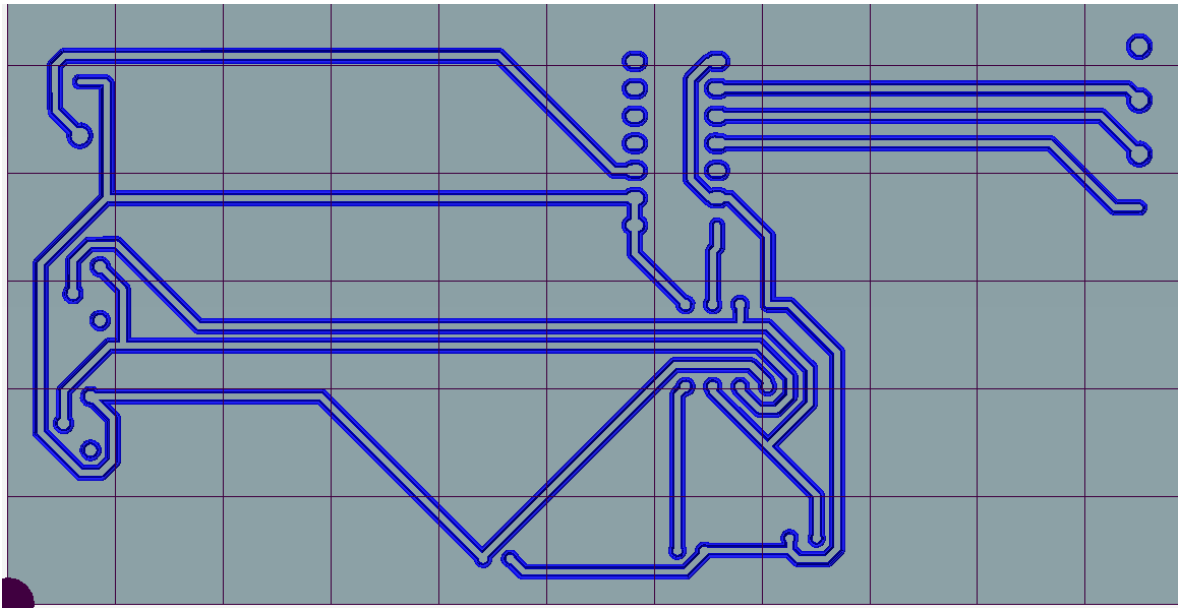


Figure 18: FM3D chip section

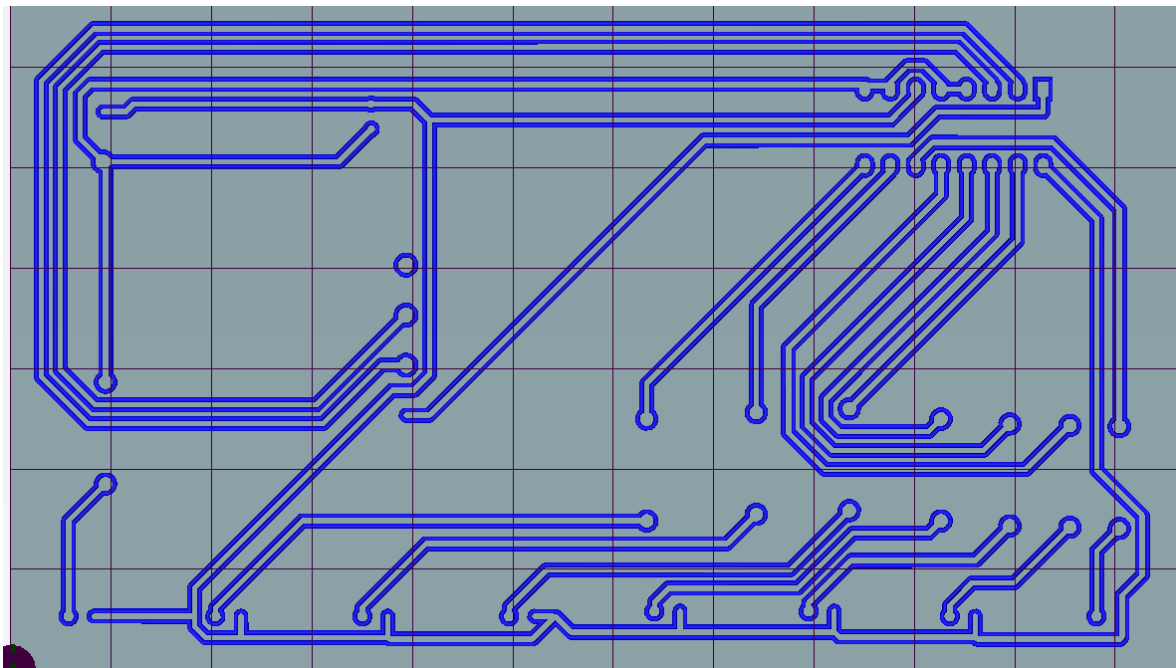


Figure 19: FM3D light section

The setting used are scan velocity is at 50mm/min, travel velocity at 300mm/min, etch current at 20mA, pump speed at 1200cc/min and 10 cuts/run. The esteemed run time for the program over the power section is 2h:5m:0s, for the circuit chips its 5h:20m:50s and for the light its 10h:41m:27s.

Result and Discussion

Concentration of the Electrolytes

The optimal concentration of the electrolytes discussed in experimental section is presented in Table 1 below. As hinted earlier the mass of salt was varied (20g, 40g, 80g, 160g, 200g, and 240g) in a fixed volume (800ml) water .

Table 2: Optimal Concentration of Electrolytes

Salt (g) in 0,8L H ₂ O	Time (sec)	Material/cut (um/cut)	Cuts (Rounds X 10)	Rounds
20	9325,00	2	250	25
40	4476,00	4.2	120	12
80	2611,00	7	70	7
120	1492,00	13	40	4
160	1492,00	13	40	4
200	1119,00	17	30	3
240	1119,00	17	30	3

In the Table, 3rd column, the “Material /cut” represents the depth of line or copper material removed per concentration per etch passage. The “Cuts” is the total number of etch passages to cut through the 0.5mm thick copper plate. The “Rounds” is the number of repetitions the program was restarted. This is due to the restriction in the software settings. The maximum value of “number of etch passages” is 10 in the tool. It is also important to emphasize that the same nozzle size was used for this operation.

Figure 20 shows the line plot of the experiment. From the result, it is obvious that the optimal concentration of the electrolytes is 200g/800ml solution. This value agrees with the manufacturer's recommendation. Hence, onward, the concentration of the electrolytes used in this work is 200g/800ml mixture.

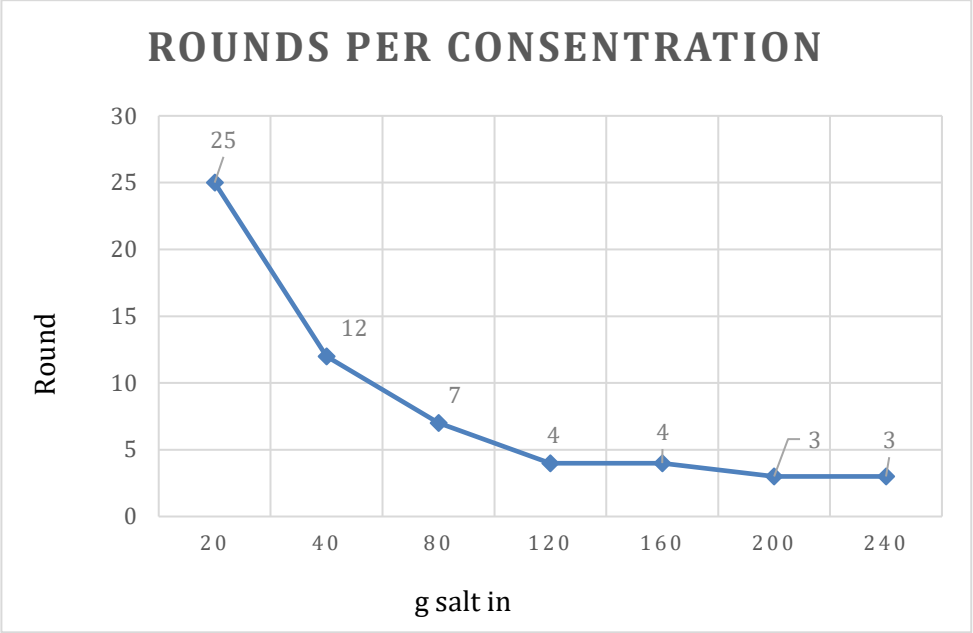


Figure 20: Rounds of program to penetrate 0,5mm copper at a given salt concentration.

Efficacy of the Electrolytes

For repeatability and consistency, the experiment was run repeated as hinted in the experimental section without changing the solution.

Table 3: Efficacy of the electrolyte after multiple use.

Repetition (Rounds = Repetition x 10)	Material Cut (um) per etch passage
1	17
2	17
3	17
4	17
5	17

From this we can see that the solution doesn't lose the etching ability from reuse over time. This result implies that the electrolytes will retain its efficacy when etching the PCB and the need of replacing the electrolyte during operation is unnecessary.

I ran the plate I will use for the circuit bord through some experiments to optimise the cuts and the setting are in the digital design.

Scan Velocity and Numbers of Etch Passages

The Scan velocity and Etch passages play a prominent role in the surface finish /quality of etching. For instance, Figure 21 shows the etching result on the PCB using untuned value of scan velocity and number of etch passages. After multiple trial and errors, it was found that the appropriate scan velocity for having better quality etch on the PCB is above 50 **mm/min**. This value represents the maximal possible value from the software.



Figure 21:Initial Etch result using default Scan Velocity and low number etch passage.

On the other hand, increasing the scan velocity to this value implies that the number of etch passages must increase as well for effective isolation of the etch lines. It would have been desirable to have the option of increasing the number of etch passages above value '10' in the software. As discussed earlier, the sequence of etching plays a significant role in the quality of etching. For further discussion, two sequence of etching a trace is established. The first is "Complete" while the other is "Partial". Complete etch can be defined as isolating a particular trace before moving to the next for a given job. For instance, using the example in Figure 12, Complete etch would be isolating the trace A before proceeding to B. Increasing the number of

etch passages would increase the likelihood of a complete etch. On the other hand, partial etch can be defined as moving interrupting the complete isolation of a particular trace during etching operation. Using the same example (A&B traces), this would imply moving intermittently between both traces during the operation. Realistically, this is achieved by setting too low value for the number of etch passages. This happens as the operator needs to re-run the sequence of operation again due to insufficient isolation of the traces.

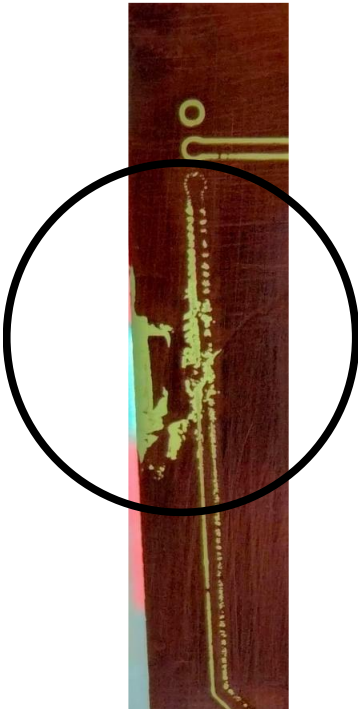


Figure 22: Possible Effect of low Scan velocity and Partial Etching.

Figure 22 (black circle) shows the effect of partial etching of the PCB. There could be several reasons for this anomaly in etching. This could be due to the undesired vibration in the FM3D during operation. Also, another reason could be the remodification of the PCB surface. Also, this might be attributed inherit with the PCB. To test the last hypothesis an AFM study was conducted on the PCB.

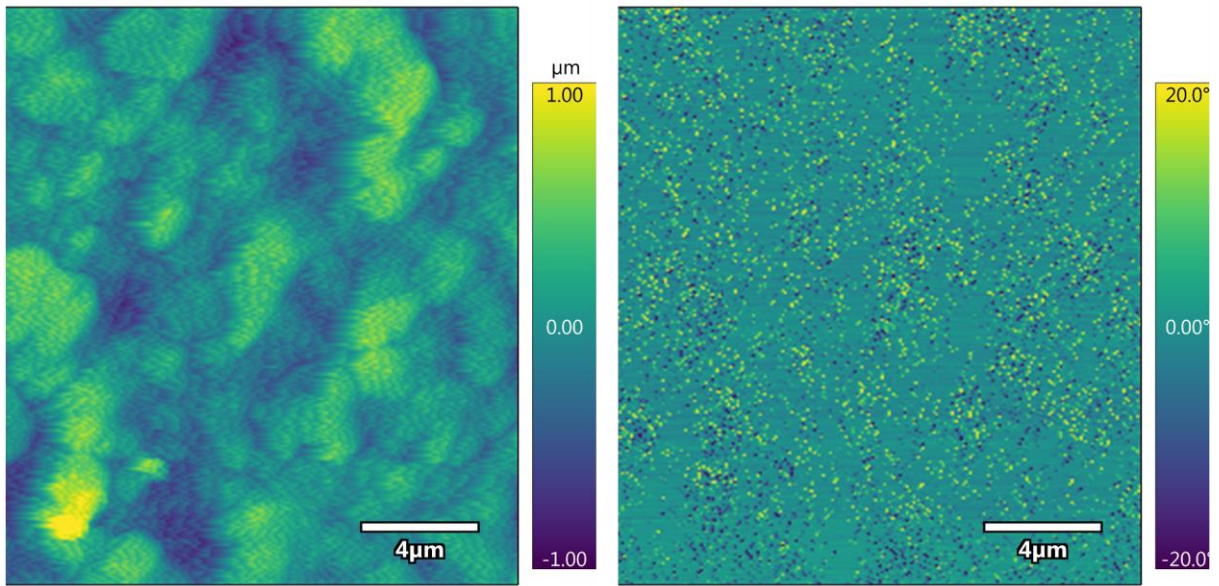


Figure 23: AFM images of PCB surface. Topography (Right) Phase Change (Left).

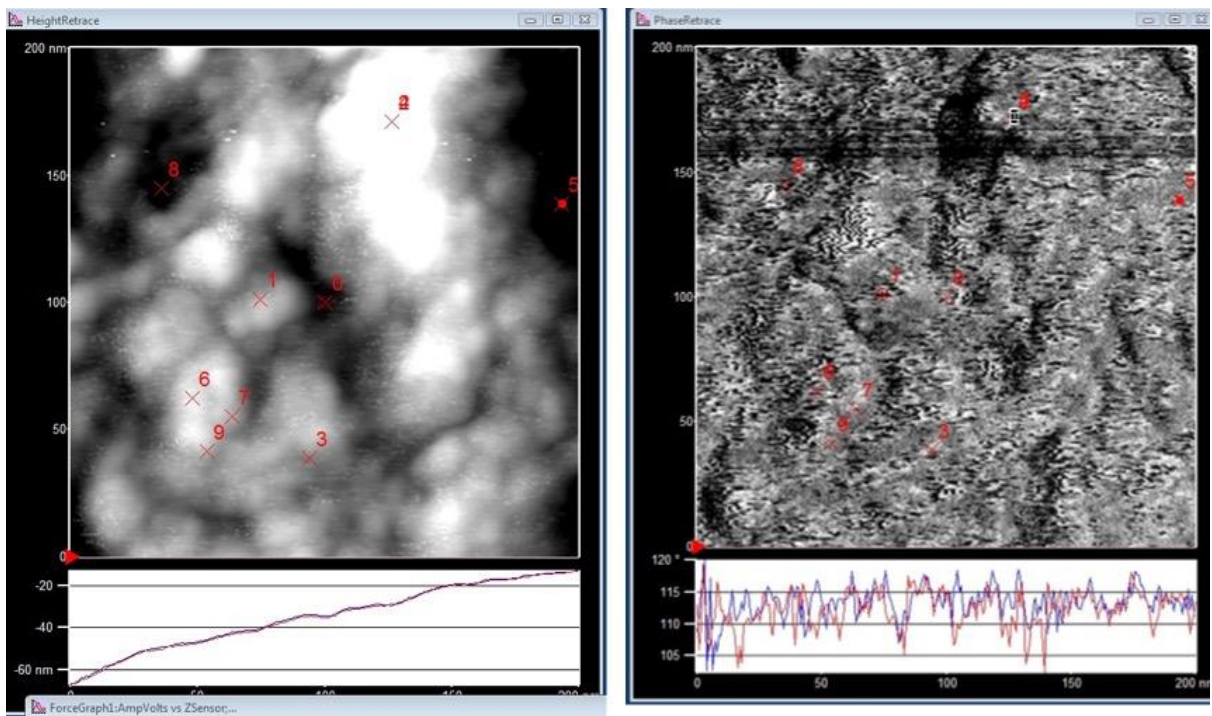


Figure 24: AFM image used in quantifying the Surface roughness and Chemical heterogeneity.

Table 4: Force curves for Figure 24.

Data category	FAD	Standard Deviation
Point 0	7.21156E-10	9.99676E-11
Point 1	5.30995E-10	1.33046E-10
Point 9	1.62376E-09	1.53494E-10
Point 2	4.24754E-09	4.46181E-10

The AFM setup was carried out on a PCB. The PCB was prepared as described in the experimental setup earlier. The AFM experiment was conducted to determine the force of adhesion (FAD) on the surface of the PCB. Basically, the FAD is the force between the tip of a probe and point of interest in the study [73, 74]. The value can be defined as

$$FAD = 4\pi R\gamma \quad \text{Equation 1}$$

Where R is the radius of the tip and γ is the surface energy. In this equation, keeping the tip radius constant, it is possible to determine the chemical homogeneity of the PCB surface. As evidence from Table 4, it is obvious that the PCB surface shows different chemical property or surface energy. The surface energy on the other hand can influence the rate of the wettability of the electrolyte of the PCB surface [75]. The role of wettability and electrochemical reaction has been established in some work [76]. Without going in-depth, it is understandable that for a given experimental setup, the rate of etching on the PCB surface might be unequal. Figure 23 is AFM image for the PCB at (20 μm x 20 μm). The size of the image is at similar scale to the nozzle tip. As it is evident in the image, chemical heterogeneity can be observed on the image.

The implication of this result is that the PCB surface has chemical heterogeneity. Consequently, requiring high number of etch passages. Also, the low scan velocity leads to poorer surface finishing. Hence, this prompted the need to using high scan velocity and high number of etch passage. The result of the PCB etching are presented.

FM3D Result

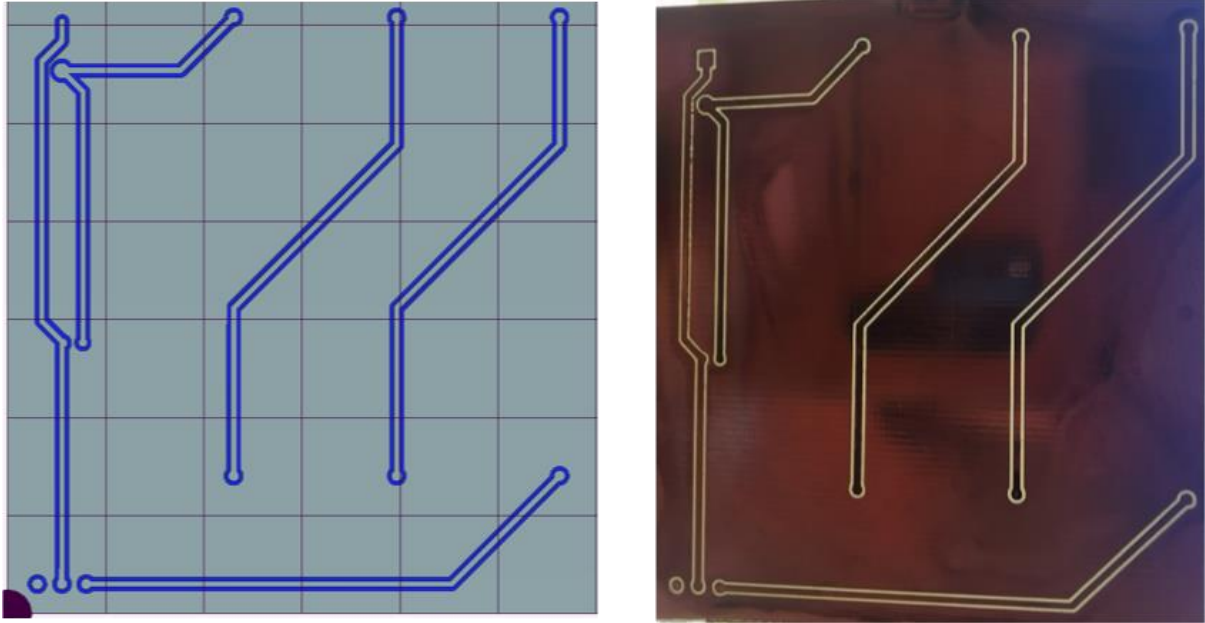


Figure 25: Battery Power Circuit. Digital copy (Left) FM3D traces (Right)

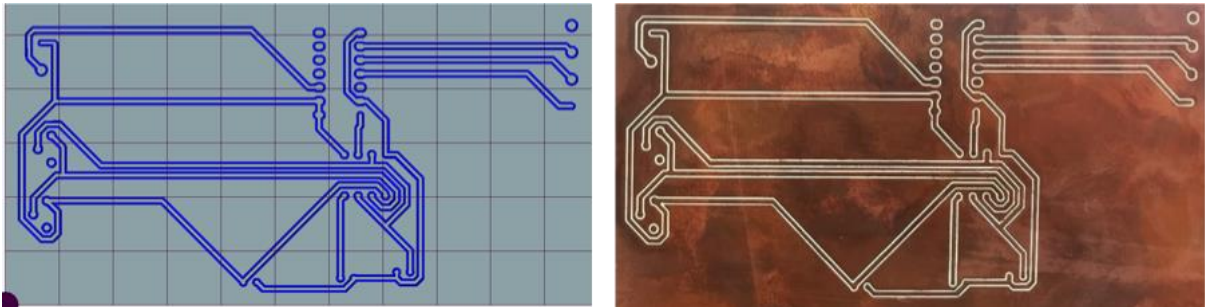


Figure 26: Chip section. Digital copy (Left), FM3D traces (Right)

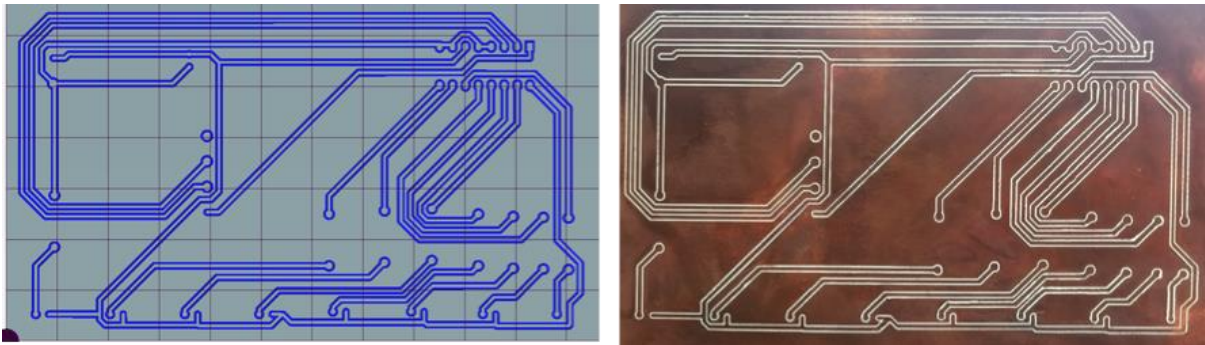


Figure 27: Lighting Circuit. Digital copy (Left). FM3D traces (Right)

LPKF Results

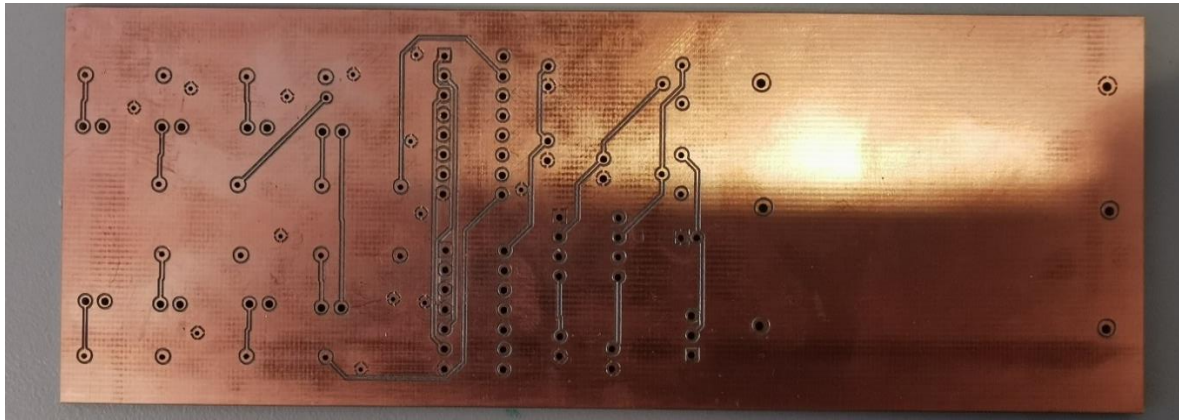


Figure 28: Top of LPKF protomat s62 magic wand.

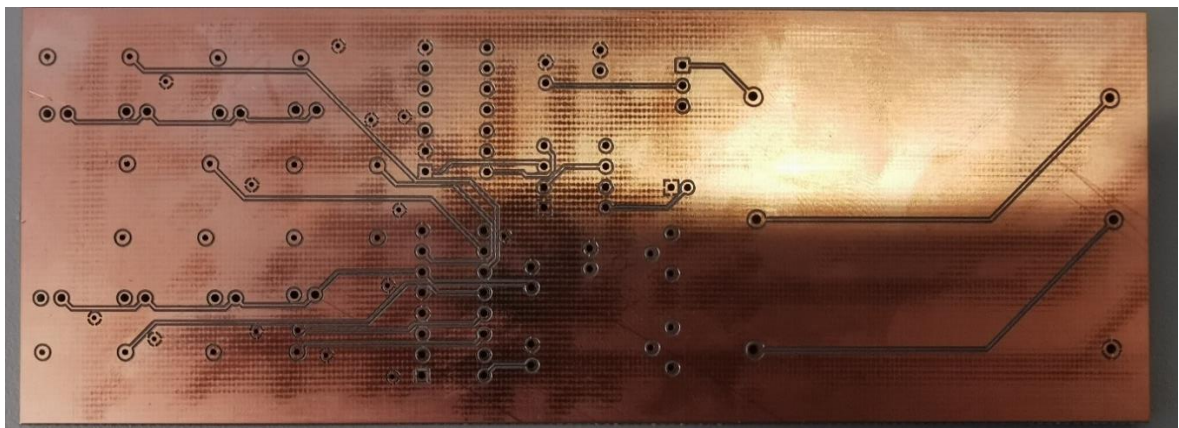


Figure 29: Bottom of LPKF protomat s62 magic wand

Evaluation

In the LPKF process took about 1 hour and the FM3D took a total of 18 hours (redesigned circuit). However

Effective Isolation: With the appropriate settings both systems (LPKF and FM3D) successfully isolated the traces of the PCB. In this respect the FM3D can be used as an alternative of the LPKF.

Quality of trace/Isolation: The quality of isolation is also satisfactory for both systems. The caveat though for is that appropriate Scan velocity and number of etch passages affects the quality of trace

Quality of surface finishing: Similarly, the quality of surface finishing from both system is also satisfactory from inspection.

Post processing: The PCB from the FM3D requires post processing to get rid of the oxidize or corroded layer. Using simple household cleaning agent, this layer can be eradicated. While there is a cost associated with sourcing the cleaning agent, it shouldn't be a deterrent in utilizing the machine in PCB processing.

Ease of drilling holes: The LPKF comes install with automatic drilling systems and tool. In this respect, PCB from the LPKF comes out with the required drilled hole. PCB from the FM3D doesn't come with the drilled hole. Also, it is challenging drilling holes manually. This will require sourcing an elaborate drilling system to support this function. This system comes at a cost that need to be factored when procuring this system.

Ease of soldering: It was challenging soldering electronic components on PCBs from both systems. For successfully soldering, the need for elaborate and high-precision soldering station is mandatory for both systems.

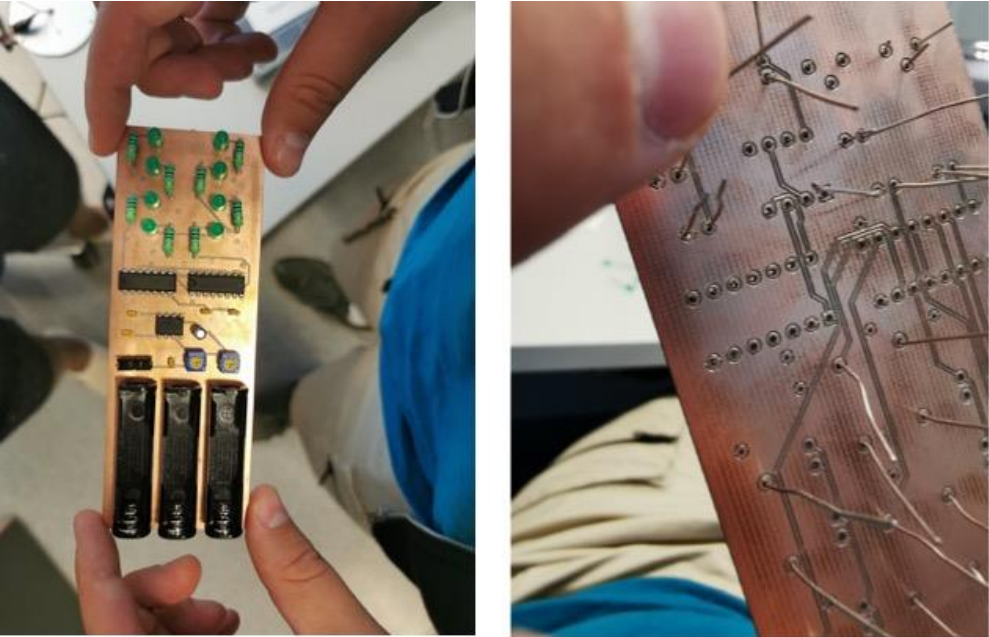


Figure 30: Assembly of components on PCB.

Conclusion

The performances of the PCBs from an electrochemical 3D printer and a commercial PCB milling machine were evaluated. The electrochemical 3D printer used is assembled using the add-on kits from Fluid Metal 3D (FM3D) and a desktop Geeetech 3D printer. The commercial PCB milling system is the LDKF ProtoMat S6 (LDKF). The basis for comparison are on ease of effective isolation, quality of traces/isolation, quality of surface finishing, post processing, ease of drilling the holes and ease of soldering. In all parameters, both systems performed at par except for few. The difference in both PCBs are, the PCB from the FM3D requires post processing in removing the oxidized layers. Also, there is the additional requirement for an elaborate drilling system for the FM3D's PCB.

However, the result of the FM3D is heavily influenced by the concentration of the electrolytes, the scan velocity, and the number of etch passages. The optimal concentration for the electrolytes is 200g of salt and 800ml of water. Also (using the process of trial and error) it was concluded that the optimal scan velocity for the FM3D should be greater than 50 mm/min for effective etching of the PCB used in this work. Effective PCB etching implies consistent isolation of the traces on the PCB. It should be noted that this setting (scan velocity) could be job-related. The reason why the scan velocity could be job related is due to the chemical heterogeneity observed during the AFM experiment. Hence, it is recommended that the appropriate scan velocity that ensures consistent etch line should be investigated before etching. Also, sequences of running the etch passages is important. It is recommended that the chosen value should be high enough that a particular trace should be completed before moving to the next trace line.

Finally, with the appropriate settings, the performance of the PCB from processes (both chemical and mechanical) are similar.

Appendix 1

FLUID METAL 3D ETCHER				
CHECK LIST FOR UNASSEMBLED UNITS				
Item group	Description	Quantity	Notes	Check
Etcher structure	Geeetech 3D printer	1	Packed separately	
Electronics box	Acrylic front panel	1		
	Acrylic back panel	1		
	Acrylic left side panel	1		
	Acrylic right side panel	1		
	Acrylic top panel	1		
	Acrylic bottom panel	1		
	Nylon screws M2 x 10	6		
	Nylon nuts M2	6		
	Box bracket	1		
	Screw M3x16	1		
	Nut M3	1		
	DB9 cable – male	1		
	DB9 connector – female	1		
	M3 x 6 screws	2		
	M3 nuts	2		
	Display	1		
	Display cable	1		
	PCB board	1		
	Broad bracket left	1		
	Broad bracket right	1		
	Nylon screws M3x12	4		
	Nylon nuts M3	4		
	Flick switch	1		
Banana connector female - red	1		Plugged onto contactor bar	
Banana connector female - black	1		Plugged onto filter	
Tray and supports	Tray supports - front	2	Shorter piece	
	Tray supports - back	2	Taller piece	
	Screws M3x16	4	Included with Geeetech	
	Nuts M3	4	Included with Geeetech	
	Tray	1		
	Barb straight - half	1		
	Nylon nut	1		

	Rubber washer	2			
	Plate	1			
	C-clamps 3.5mm	7			
	C-clamps 4.5mm	7			
Contactorm arm	Contactorm arm	1			
	Screw nylon M4x16	1			
	Nut nylon M4	1			
	Washer M4	1			
Nozzle	Nozzle	4			
	Mock nozzle	1			
Filter	Filter bottle with filter	1	Assembled		
	Filter bottle top cap	1			
	Filter top cap rubber ring	1			
	Filter bottle bottom cap	1			
	Filter bottom cap rubber ring	1			
	Filter support	1			
	Air cannon	1			
	Fan	1	Included with Geeetech		
	Fan extension cable	1	Included with Geeetech		
	Screws M4x16	2			
	Nuts M4	2			
	Piping	Water tank	1		
		Barb L shape	1		
Barb straight		1			
Nylon nut M8		2			
Rubber washer M8		2			
Silicone tube 32cm		1	Valve to pump		
Silicone tube 5cm		1	Water tank to valve		
Valve		1			
Silicone tube 26cm		1	Pump to filter bottle		
Silicone tube 47cm		1	Tray to water tank		
Zip ties		15			
Pump	Motor	1			
	Pump	1			
	Pump bracket part A	1			
	Pump bracket part B	1			
	Screws M4x20	2			
	Nuts M4	2			
	Screws M3 x 8 flat head	4			
End stops	X trigger	1			
	Screw M4x16	1			
	Y trigger	1			
	Screw M4x16	1			
	Y end stop	1			
	Screws M2.5x18	2			

	Nuts M2.5	2	
	Z adjustment	1	
	Z trigger	1	
	Screw M3x35	1	Included with Geeetech
Safety box	H joint	2	
	Nylon screws M3x12	4	
	Nylon nuts M3	4	
	Corner H joint	2	
	Hinge part A	2	
	Hinge part B	2	
	Nylon screws M3x20	2	
	Nylon nuts M3	2	
	Nylon screws M2.5x12	2	
	Nylon nuts M2.5x12	2	
	Safety Switch	1	
	Nuts M10	2	
	Acrylic front part - side panel left	1	
	Acrylic front part - side panel right	1	
	Acrylic front part - front panel	1	
	Acrylic front part - lid panel A	1	
	Acrylic front part - lid panel B	1	
	Acrylic back part - side panel left	1	
	Acrylic back part - side panel right	1	
	Acrylic back part - top panel	1	
	Acrylic back part - back panel	1	
	Locking clips	2	Included with Geeetech
	Nylon screws M3x12	12	
Nylon nut M3	12		
Nylon washer M3	12		
Etcher supports	Etcher supports	2	

APPENDIX 2



6. Operation Instructions

Before following the operation instructions, make sure you follow the Installation instructions thoroughly.

1. Add the electrolyte

- Mix 200grams of table salt with 800ml of water.
- Fill the water tank with the solution.

2. Place your PCB board or metal piece

(For further assistance, please check video [8.Placing_metal_sheet_PCB.mp4](#))

- Manually lift the Z axis by rotating the shafts. Make sure that the X axis remains parallel to the frame of the Etcher.
- Before placing your PCB board or metal piece onto the plate, plan where the contactor arm should be positioned based on your design. This is so the nozzle or air cannon do no crash into it or move it while etching.
- Place your PCB board or metal piece on the plate and align it to the front left corner (This is position x0,y0).
- Secure it with the C-clamps. Use the 3.5mm clamps for parts up to 1mm thick or the 4.5 mm clamps for parts up to 2mm thick.
- For odd shaped or thicker than 2mm pieces you may use cellotape. If you do so, make sure it is not placed anywhere the nozzle will pass through or where the contactor arm will be touching your piece.
- Slide the contactor arm above your piece. Make sure the pin makes good contact with the metal surface.

3. Check the filter bottle

- Make sure both caps are tightly secured to the filter bottle to avoid any leakage.

4. Install the nozzle (If not already installed or to replace broken nozzle)

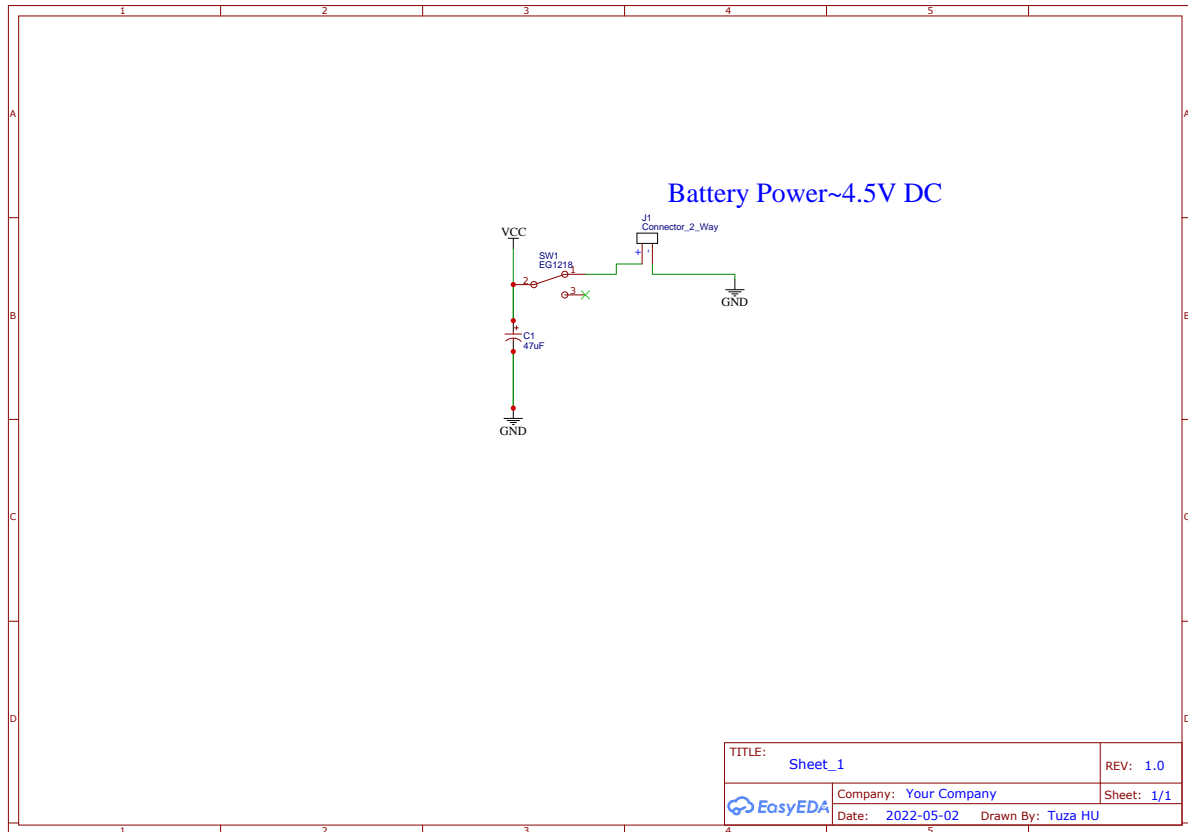
(For further assistance, please check video [9.Inserting_the_nozzle.mp4](#))

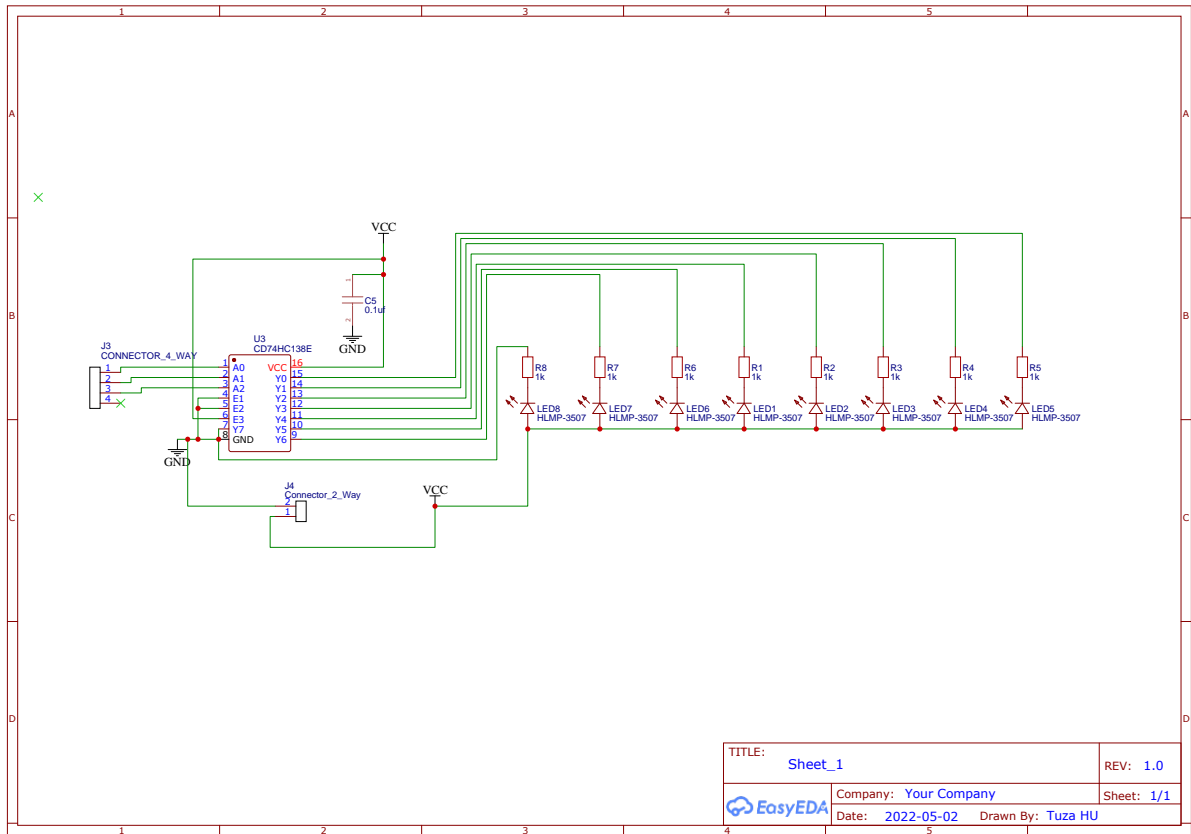
- Remove the filter bottle from the filter support by unscrewing.
- Remove the bottom cap of the filter bottle and take out the rubber ring.
- Carefully place in the cap the cone with the nozzle.
- Place the rubber ring on top.
- Press the rubber ring all around to make sure it makes good contact.
- Screw the bottom cap back onto the filter bottle.
- Make sure it is tight enough to avoid leakage during etching

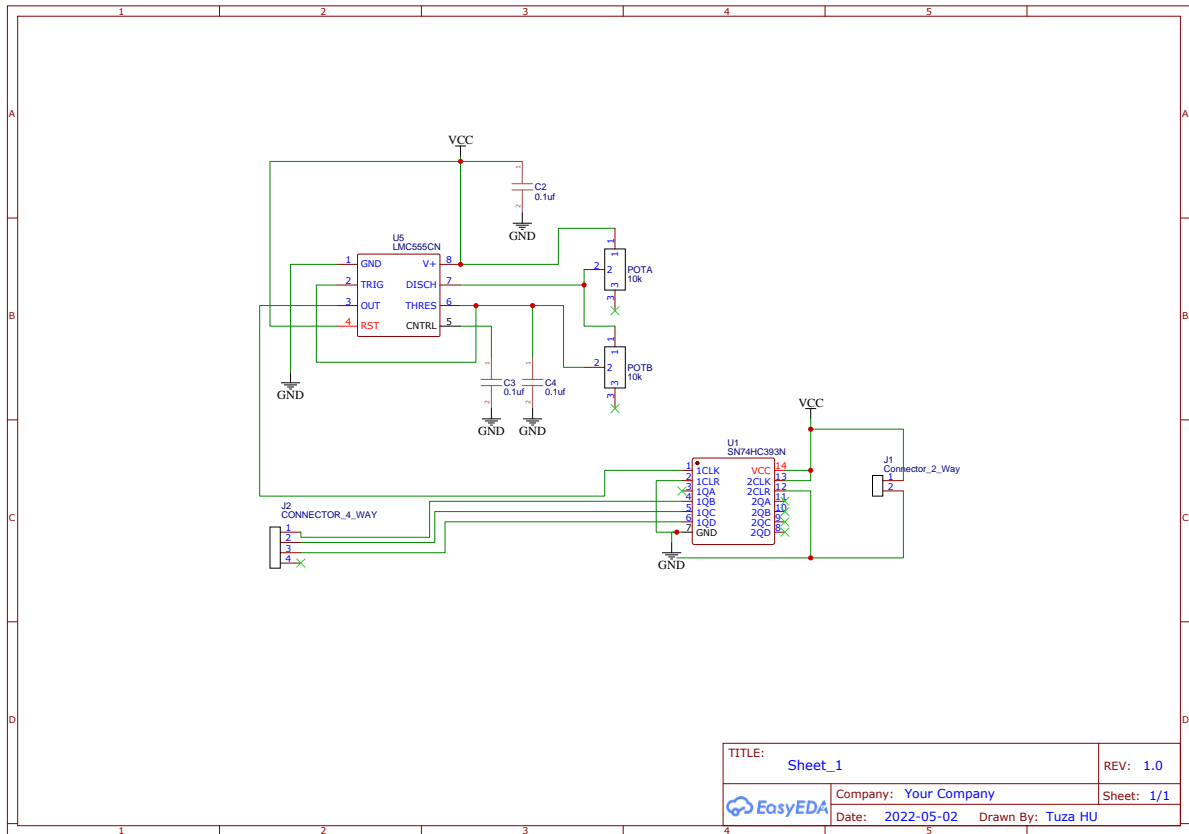
Appendix 3: Part List for Magic Wand

Components	Rating	Quantity (no)
AAA Battery Holder	1.5 A	3
Capacitor	0.1uF	1
Capacitor	1000pF	5
LED green		8
Ohm resistor		8
Switch		8
CMOS Timer		1
Counter/Divider		1
Decoder/Demultiplexer		1
Electrolytic Capacitor	47uf	1

Appendix 4: Modified Schematic for FM3D







TITLE:	Sheet_1	REV:	1.0
Company: Your Company		Sheet: 1/1	
EasyEDA		Date: 2022-05-02	Drawn By: Tuza HU

Reference

1. Mukhtarkhanov, M., A. Perveen, and D. Talamona, *Application of stereolithography based 3D printing technology in investment casting*. *Micromachines*, 2020. **11**(10): p. 946.
2. Bharat Bhushan, M.C. *An overview of additive manufacturing (3D printing) for microfabrication*. 2017; Available from:
<https://link.springer.com/content/pdf/10.1007/s00542-017-3342-8.pdf>.
3. Yong He, G.-h.X., Jian-zhong Fu. *Fabrication of low cost soft tissue prostheses with the desktop 3D printer*. 2014; Available from:
<https://www.nature.com/articles/srep06973>.
4. Sunil C. Joshi, A.A.S. *3D printing in aerospace and its long-term sustainability*. 2015; Available from:
https://www.tandfonline.com/doi/full/10.1080/17452759.2015.1111519?casa_token=5FINWHcEJEwAAAAA%3AIO6NbdKgXyGnJJxQT6PlzpxEFflnGTjn1G5TpC46ZS-uj68cgLM5UF7cC8h40kinUs7ZI40jwwjw.
5. Jie Sun, Z.P., Weibiao Zhou, Jerry Y.H. Fuh, Geok Soon Hong, Annette Chiu. *A Review on 3D Printing for Customized Food Fabrication*. 2015; Available from:
<https://www.sciencedirect.com/science/article/pii/S2351978915010574>.
6. Qian Yan, H.D., Jin Su, Jianhua Han, Bo Song, Qingsong Wei, Yusheng Shi. *A Review of 3D Printing Technology for Medical Applications*. 2018; Available from:
<https://www.sciencedirect.com/science/article/pii/S2095809917306756>.
7. Prakash, K.S., T. Nancharaih, and V.S. Rao, *Additive manufacturing techniques in manufacturing-an overview*. *Materials Today: Proceedings*, 2018. **5**(2): p. 3873-3882.

8. Lu, B., H. Lan, and H. Liu, *Additive manufacturing frontier: 3D printing electronics*. Opto-Electronic Advances, 2018. **1**(1): p. 170004-170004.
9. Tang, H.-H., M.-L. Chiu, and H.-C. Yen, *Slurry-based selective laser sintering of polymer-coated ceramic powders to fabricate high strength alumina parts*. Journal of the European Ceramic Society, 2011. **31**(8): p. 1383-1388.
10. Kamrani, A.K. and E.A. Nasr, *Engineering design and rapid prototyping*. 2010: Springer Science & Business Media.
11. Anderson, J., *Advantages and disadvantages of laser stereolithography*. Ezin Articles. 2007.
12. Halloran, J.W., et al., *Photopolymerization of powder suspensions for shaping ceramics*. Journal of the European Ceramic Society, 2011. **31**(14): p. 2613-2619.
13. Kruth, J.-P., M.-C. Leu, and T. Nakagawa, *Progress in additive manufacturing and rapid prototyping*. Cirp Annals, 1998. **47**(2): p. 525-540.
14. Chen, X., et al., *A low cost desktop electrochemical metal 3D printer*. Advanced Materials Technologies, 2017. **2**(10): p. 1700148.
15. Rother, M., et al., *Aerosol-Jet Printing of Polymer-Sorted (6, 5) Carbon Nanotubes for Field-Effect Transistors with High Reproducibility*. Advanced Electronic Materials, 2017. **3**(8): p. 1700080.
16. Dasgupta, S., et al., *Inkjet printed, high mobility inorganic-oxide field effect transistors processed at room temperature*. ACS nano, 2011. **5**(12): p. 9628-9638.
17. Fukuda, K. and T. Someya, *Recent progress in the development of printed thin-film transistors and circuits with high-resolution printing technology*. Advanced materials, 2017. **29**(25): p. 1602736.
18. Gaikwad, A.M., et al., *A flexible high potential printed battery for powering printed electronics*. Applied Physics Letters, 2013. **102**(23): p. 104_1.

19. Giannakou, P., et al., *Energy storage on demand: ultra-high-rate and high-energy-density inkjet-printed NiO micro-supercapacitors*. Journal of Materials Chemistry A, 2019. **7**(37): p. 21496-21506.
20. Grande, L., et al., *Graphene for energy harvesting/storage devices and printed electronics*. Particuology, 2012. **10**(1): p. 1-8.
21. Cao, Z., et al., *Flexible screen printed thermoelectric generator with enhanced processes and materials*. Sensors and Actuators A: Physical, 2016. **238**: p. 196-206.
22. Han, T., et al., *3D printed sensors for biomedical applications: a review*. Sensors, 2019. **19**(7): p. 1706.
23. Carter, J.C., et al., *Fabricating optical fiber imaging sensors using inkjet printing technology: A pH sensor proof-of-concept*. Biosensors and Bioelectronics, 2006. **21**(7): p. 1359-1364.
24. Reddy, A., et al., *Printed capacitive based humidity sensors on flexible substrates*. Sensor Letters, 2011. **9**(2): p. 869-871.
25. Niu, S., et al., *A wireless body area sensor network based on stretchable passive tags*. Nature Electronics, 2019. **2**(8): p. 361-368.
26. Rivadeneyra, A., et al., *Design and characterization of a low thermal drift capacitive humidity sensor by inkjet-printing*. Sensors and Actuators B: Chemical, 2014. **195**: p. 123-131.
27. Subramanian, V., et al., *Progress toward development of all-printed RFID tags: materials, processes, and devices*. Proceedings of the IEEE, 2005. **93**(7): p. 1330-1338.
28. Guo, S.Z., et al., *3D printed stretchable tactile sensors*. Advanced Materials, 2017. **29**(27): p. 1701218.

29. Vena, A., et al., *A fully inkjet-printed wireless and chipless sensor for CO₂ and temperature detection*. IEEE Sensors Journal, 2014. **15**(1): p. 89-99.
30. Yue Xu, C.D., *An investigation on 3D printing technology for power electronic converters*. 2022.
31. Vivek Muthu, P.C., Tseng King Jet. *Review on application of additive manufacturing for electrical power converters*. 2016; Available from:
<https://ieeexplore.ieee.org/abstract/document/7848445>.
32. U. Kalsoom, A.P., P.N. Nesterenko, B. Paull, *A 3D printable diamond polymer composite: a novel material for fabrication of low cost thermally conducting devices*. 2016.
33. Madhu Chinthavali, C.A., Steven Campbell, Randy Wiles, Burak Ozpineci. *A 10-kW SiC inverter with a novel printed metal power module with integrated cooling using additive manufacturing*. 2014; Available from:
<https://ieeexplore.ieee.org/abstract/document/6964622>.
34. Rhys Owen Jones, P.I., Adrian Bowyer. *Rapid manufacturing of functional engineering components*. 2012; Available from:
<https://researchportal.bath.ac.uk/en/publications/rapid-manufacturing-of-functional-engineeringcomponents>.
35. David Reay, R.M., Peter Kew. *Heat pipes: Theory, design and applications*. 2014; Available from:
https://books.google.no/books?hl=no&lr=&id=_G2SIYmFLEAC&oi=fnd&pg=PP1&dq=Heat+pipes:+Theory,+design+and+applications&ots=L8N38N42sJ&sig=lzMNibJZXe-cV-3vyCA6ddBGKDI&redir_esc=y#v=onepage&q=Heat%20pipes%3A%20Theory%2C%20design%20and%20applications&f=false.

36. Flowers, P.F., et al., *3D printing electronic components and circuits with conductive thermoplastic filament*. Additive Manufacturing, 2017. **18**: p. 156-163.
37. Liang, M., et al., *3-D printed microwave patch antenna via fused deposition method and ultrasonic wire mesh embedding technique*. IEEE Antennas and Wireless Propagation Letters, 2015. **14**: p. 1346-1349.
38. Espalin, D., et al., *3D Printing multifunctionality: structures with electronics*. The International Journal of Advanced Manufacturing Technology, 2014. **72**(5): p. 963-978.
39. Lehmus, D., et al., *Customized smartness: a survey on links between additive manufacturing and sensor integration*. Procedia Technology, 2016. **26**: p. 284-301.
40. MacDonald, E. and R. Wicker, *Multiprocess 3D printing for increasing component functionality*. Science, 2016. **353**(6307): p. aaf2093.
41. Wicker, R.B. and E.W. MacDonald, *Multi-material, multi-technology stereolithography: This feature article covers a decade of research into tackling one of the major challenges of the stereolithography technique, which is including multiple materials in one construct*. Virtual and Physical Prototyping, 2012. **7**(3): p. 181-194.
42. Ready, S., G. Whiting, and T.N. Ng. *Multi-material 3D printing*. in *NIP & Digital Fabrication Conference*. 2014. Society for Imaging Science and Technology.
43. Wu, S.-Y., et al., *3D-printed microelectronics for integrated circuitry and passive wireless sensors*. Microsystems & Nanoengineering, 2015. **1**(1): p. 1-9.
44. Lopes, A.J., E. MacDonald, and R.B. Wicker, *Integrating stereolithography and direct print technologies for 3D structural electronics fabrication*. Rapid Prototyping Journal, 2012.

45. Jang, S.H., et al., *3-dimensional circuit device fabrication process using stereolithography and direct writing*. International Journal of Precision Engineering and Manufacturing, 2015. **16**(7): p. 1361-1367.
46. S.H Masood, W.Q.S. *Development of new metal/polymer materials for rapid tooling using Fused deposition modelling*. 10/7/2004; Available from:
<https://www.sciencedirect.com/science/article/abs/pii/S0261306904000378?via%3Dihub>.
47. A Simchi, F.P., H Pohl. *On the development of direct metal laser sintering for rapid tooling*. 11/1/2003; Available from:
<https://www.sciencedirect.com/science/article/abs/pii/S0924013603002838?via%3Dihub>.
48. Lawrence E. Murrab, S.M.G., Diana A. Ramirezab, Edwin Martinezab, Jennifer Hernandezab, Krista N. Amato, Patrick W. Shindoab, Francisco R. Medinaab, Ryan B. Wickerab. *Metal Fabrication by Additive Manufacturing Using Laser and Electron Beam Melting Technologies*. 1/1/2012; Available from:
<https://www.sciencedirect.com/science/article/abs/pii/S1005030212600164?via%3Dihub>.
49. Beth E. Carrolla, T.A.P., Allison M. Beese. *Anisotropic tensile behavior of Ti–6Al–4V components fabricated with directed energy deposition additive manufacturing*. 4/1/2015; Available from:
<https://www.sciencedirect.com/science/article/abs/pii/S135964541400980X?via%3Dihub>.
50. 3D, F.m. *Who could tell working with metal would be possible without heat, friction or expensive setups?* 9/8/2021; Available from:
<https://www.fluidmetal3d.com/technology/>.

51. J. D. Madden, I.W.H. *Three-dimensional microfabrication by localized electrochemical deposition*. 1996; Available from: https://ieeexplore.ieee.org/abstract/document/485212?casa_token=ouKwDWERwQQAAAAA:om3SbYHZ7jcVFo1yFY_4KfxG-p9aC7oBNIBEmMxZ6RWk5iB0gA0AF8ToVTePQ02wqnn0f2SaVQ.
52. Jie Hu, M.-F.y. *Meniscus-Confined Three-Dimensional Electrodeposition for Direct Writing of Wire Bonds*. 2010; Available from: https://www.science.org/doi/full/10.1126/science.1190496?casa_token=ckfM9T-pMpEAAAAA%3AVASEPwI4mV7P_YauHzu5EoLfwrTvO_O1sV-EvFGm-flFzCM-E6ekP7jxFKSX8jXxTNjaM_HI_UazrQ.
53. Yan Li, B.W.M., and Jie Liu. *Electrochemical AFM “Dip-Pen” Nanolithography*. 2001; Available from: <https://pubs.acs.org/doi/full/10.1021/ja005654m>.
54. Abhijit P Suryavanshi, M.-F.Y. *Electrochemical fountain pen nanofabrication of vertically grown platinum nanowires*. 2007; Available from: <https://iopscience.iop.org/article/10.1088/0957-4484/18/10/105305/meta>.
55. C. Buchanan, L.G. *Metal 3D printing in construction: A review of methods, research, applications, opportunities and challenges*. 2019; Available from: https://www.sciencedirect.com/science/article/pii/S0141029618307958?casa_token=J4mVoeJ0dc8AAAAA:6prQR2vPVQjYgHJYuiaFP1Kg6LTWjkJQ-T4f0fEetiivYJr5dT89KvVAJB9f8Au8QGVe0IGFyA.
56. 3D, f.m. *Fluid metal 3D*. 2022; Available from: <https://www.fluidmetal3d.com/>.
57. 3D, F.m. *Next generation metalwork and PCB making*. 2022; Available from: <https://www.fluidmetal3d.com/>.
58. Arizona State University, T., AZ. *Electrochemical Etching Improves 3D printing of metals*. 2016; Available from:

- <https://www.medicaldesignbriefs.com/component/content/article/mdb/supplements/mf/briefs/25537>.
59. Keulegan, G.H., *Hydrodynamics of cathode films*. Journal of Research of the National Bureau of Standards, 1951. **47**(3): p. 156.
 60. 3D, f.m. *Hassle free and easy etching from your desk*. 9/8/2021; Available from: <https://www.fluidmetal3d.com/product/>.
 61. Marco, S. *Fluid metal 3D AS*. 2/4/2021; Available from: <https://worldwide.espacenet.com/patent/search/family/068653542/publication/WO2021019449A1?q=102019000013626%20>.
 62. Wikipedia. *Printed circuit board*. 2022; Available from: https://en.wikipedia.org/wiki/Printed_circuit_board.
 63. Wikipedia. *Through-hole technology*. 2022; Available from: https://en.wikipedia.org/wiki/Through-hole_technology.
 64. F., A.M.D.S. *Process of assembling electrical circuits*. 1956; Available from: <https://worldwide.espacenet.com/patent/search/family/022666303/publication/US2756485A?q=pn%3DUS2756485>.
 65. Ming-Hung Shu, C.-H.C., Jing-Rong Chang. *Using intuitionistic fuzzy sets for fault-tree analysis on printed circuit board assembly*. 2006; Available from: https://www.sciencedirect.com/science/article/pii/S0026271406000217?casa_token=U-AUkd7hiAUAAAAA:SrZUk-5Jx9knCH6-m_X6FgUZwlEyMGki-2_htGxeII6fOc2okEegrluUIItRGHgLfeyQ5Z41sA.
 66. Dou, J.L. *Printed circuit board industry*. 2016; Available from: <https://www.sciencedirect.com/science/article/abs/pii/S1438463906000204>.
 67. Voltera. *The V-One is a multi-functional circuit printer, optimizing R&D productivity at your desk*. 2022; Available from: <https://www.voltera.io/product>.

68. KayoSaat. *Semi-automatic inline screen printer, model KAYO-5088XL*. 2022; Available from: <https://www.kayosmt.eu/catalog/screen-printers-for-solder-paste/KAYO-5088XL/>.
69. Alibaba. *PCB Board Making Machine / SMT PCB Plate Making Machine Supplier from China PCB2100*. 2022; Available from: https://www.alibaba.com/product-detail/Pcb-Making-Machine-PCB-Board-Making_60102316623.html?spm=a2700.7724857.topad_classic.d_title.27522410ytOdkp.
70. Khandpur, R.S., *Printed circuit boards: design, fabrication, assembly and testing*. 2006: Tata McGraw-Hill Education.
71. AG, L.L.E. *ProtoMat® S62 Operating Manual 7.1, English*. 2008; Available from: https://www.loesbogers.com/digitalfabrication/files/ProtoMat_S62_Operating_manual_V7.1_en.pdf.
72. Lamothe, A. *Magic Wand*. 2018; Available from: <https://circuitmaker.com/Projects/Details/Andre-LaMothe/Crashcourse-Electronics-Magic-Wand#sectionDesignFiles>.
73. Israelachvili, J.N., *Intermolecular and surface forces*. 2011: Academic press.
74. Yaminsky, V., *The hydrophobic force: the constant volume capillary approximation*. *Colloids and Surfaces A: Physicochemical and Engineering Aspects*, 1999. **159**(1): p. 181-195.
75. Al Mahri, M.A., et al., *Surface alteration of calcite: interpreting macroscopic observations by means of AFM*. *Physical Chemistry Chemical Physics*, 2017. **19**(37): p. 25634-25642.
76. Li, M., et al., *The role of electrode wettability in electrochemical reduction of carbon dioxide*. *Journal of Materials Chemistry A*, 2021.

